

Magnetorheological Strut for Vibration Isolation System of Space Launcher

Author:

Ing. Ondřej Macháček

Supervisors:

Doc. Ing. Ivan Mazůrek, CSc.

Ing. Jakub Roupec, PhD.



Brno, 7 December, 2018

Content and Motivation

Content

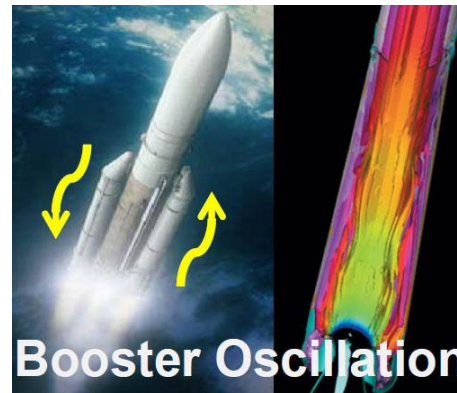
- State of art
- Aim of thesis
- Methods
- Results
 - Experimental MR strut (design, manufacture, tests)
 - MR Strut for VIS of launch vehicle (design)
- Conclusion

Spacecraft (Payload)

Vibration Isolation System (VIS)



Lift-Off blastwave



Booster Oscillation



Fairing Separation

State of art

Structural vibration isolation systems (VIS) – Payload adapters

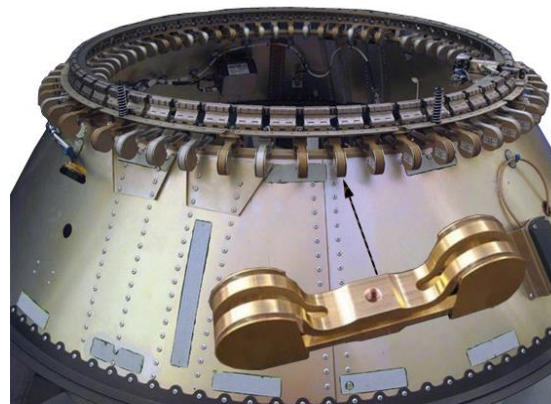
- Low efficiency → VIS based on struts

esa



[Perez, 2014]

NASA



[White, 2015]

SPACEX



[spacex.com]

State of art

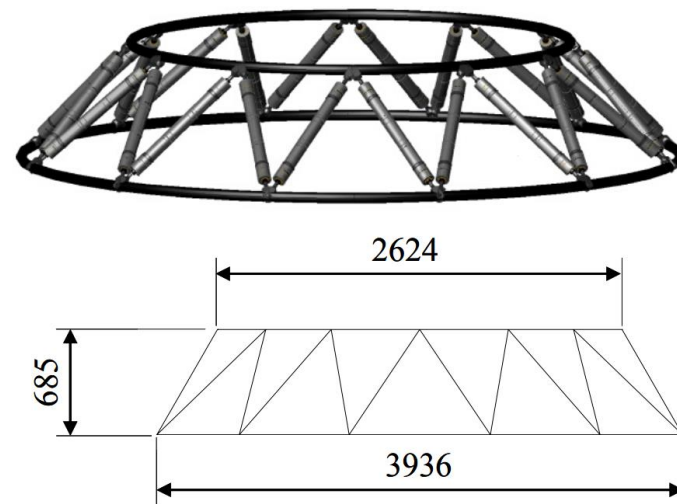
Vibration isolation systems based on struts – Stewart platform

Passive



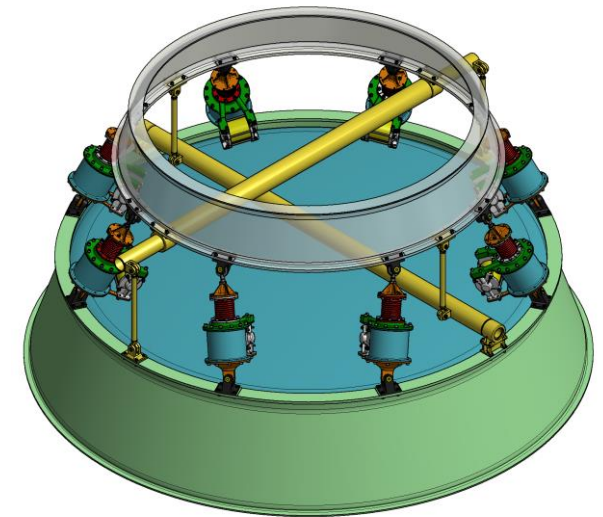
[Rubsamen, 2003]

Active



[Eilers, 2007]

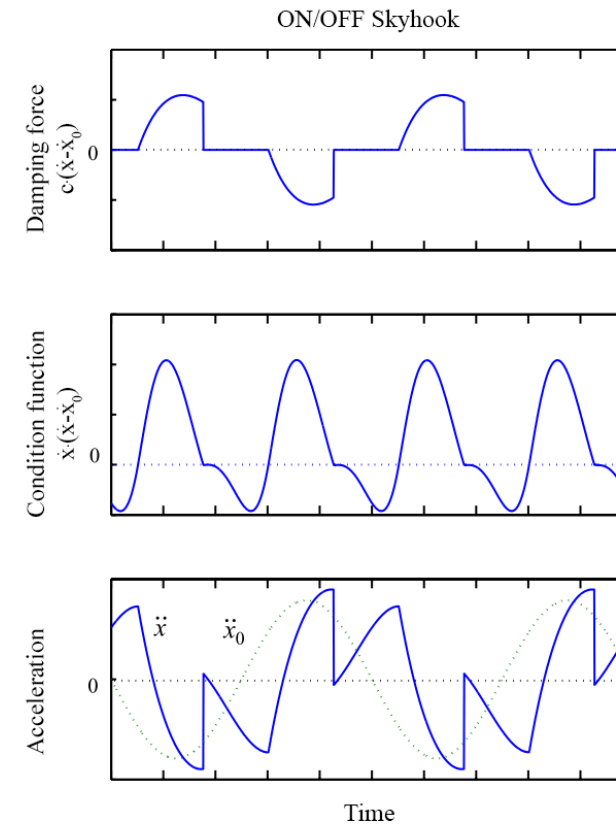
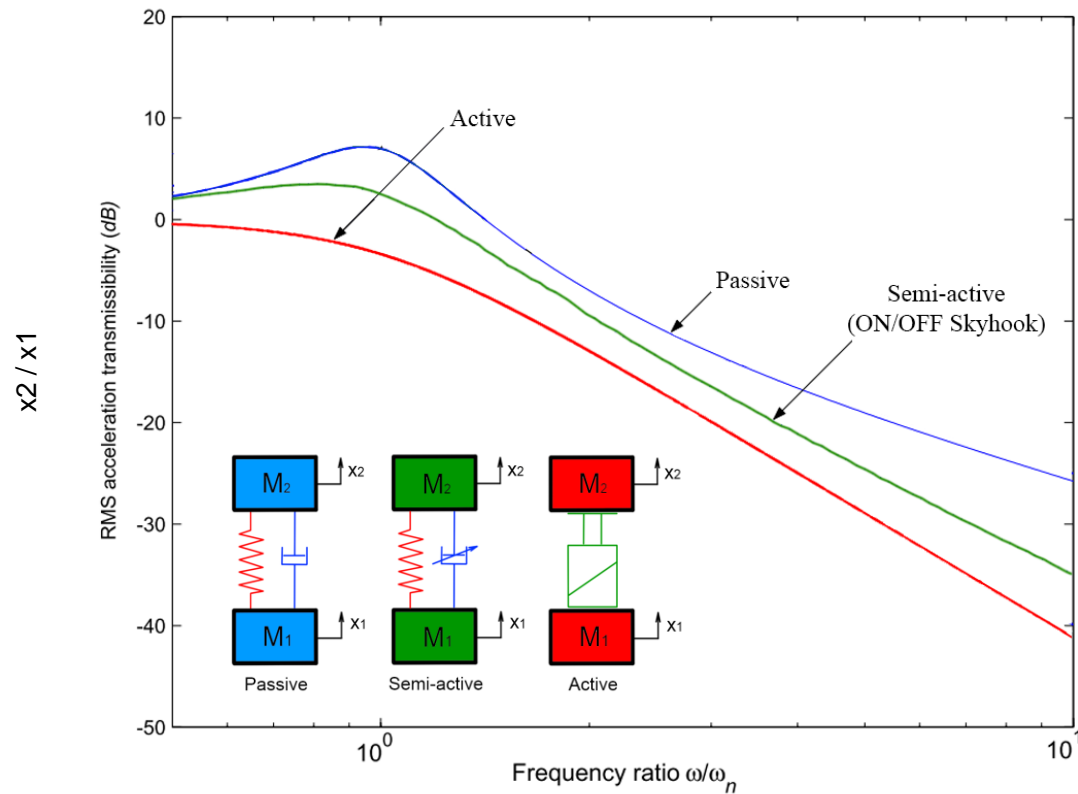
Semi - active



[esa.com]

State of art

Transmissibility comparison of Passive, Active and SA vibration isolators (axial)



[Liu, 2005]

State of art

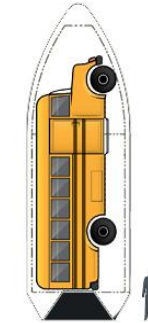
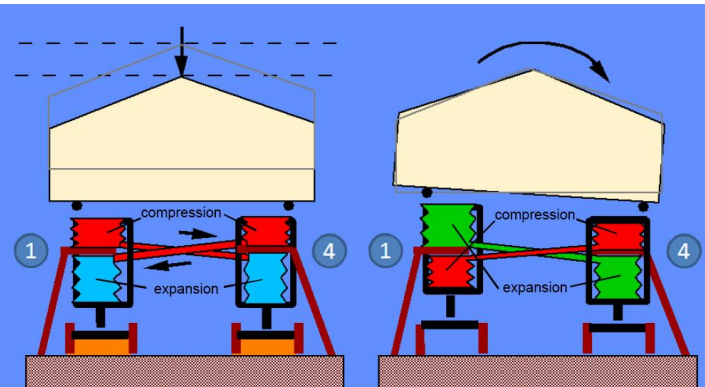
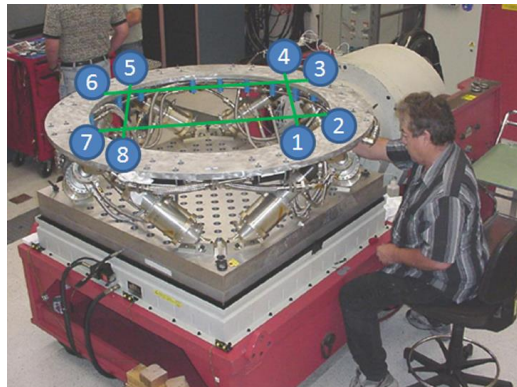
Hydraulic stabilizer of Evolved Launch Vibration Isolation System (ELVIS)

Usually shaped spacecrafts (payloads) are prone to yawing

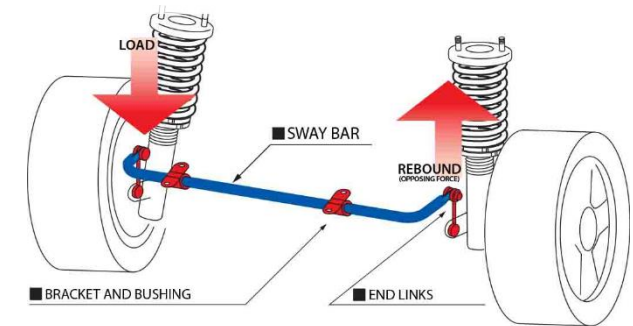
Lateral direction has to be stiffer than axial

- Strut position
- Stabilizer

High damping in axial direction



<http://www.spacex.com>



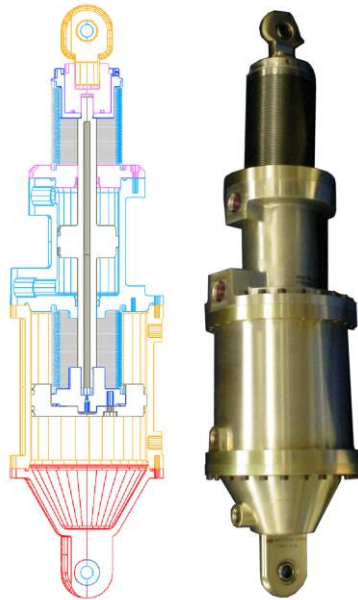
<http://www.cuscousainc.com>

[Ruebsamen, 2003]

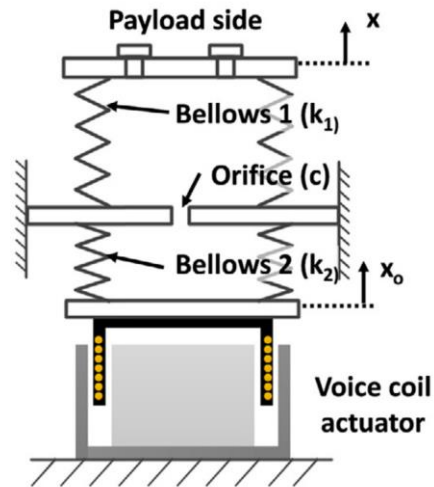
State of art

Struts of VIS for launch vehicle

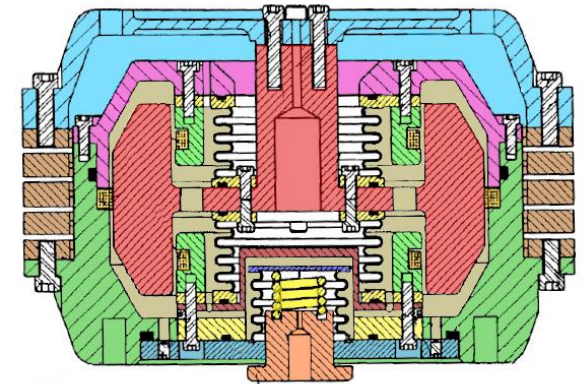
No leakage \longrightarrow unconventional sealing by elastic metal bellows



[Rubsamen, 2003]



[Lee, 2015]

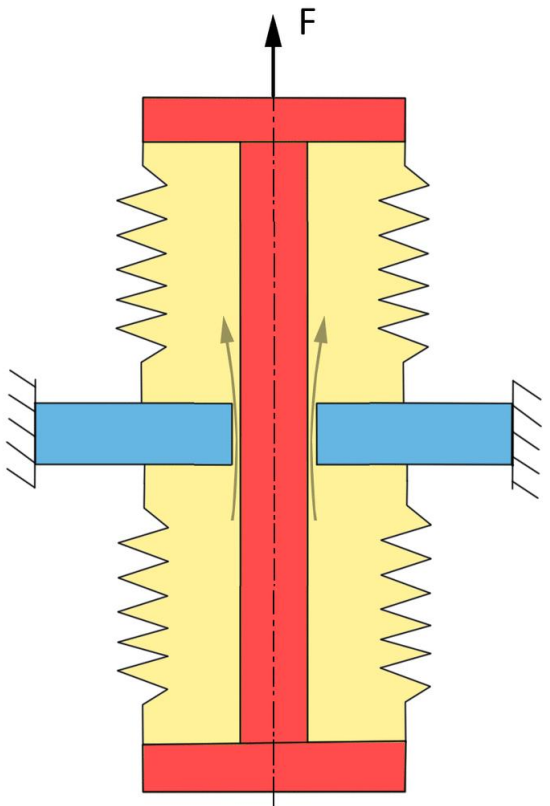


[Kelso, 2004]

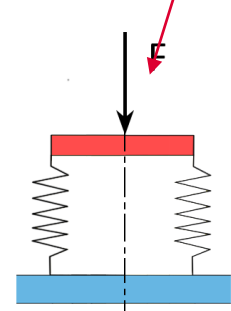
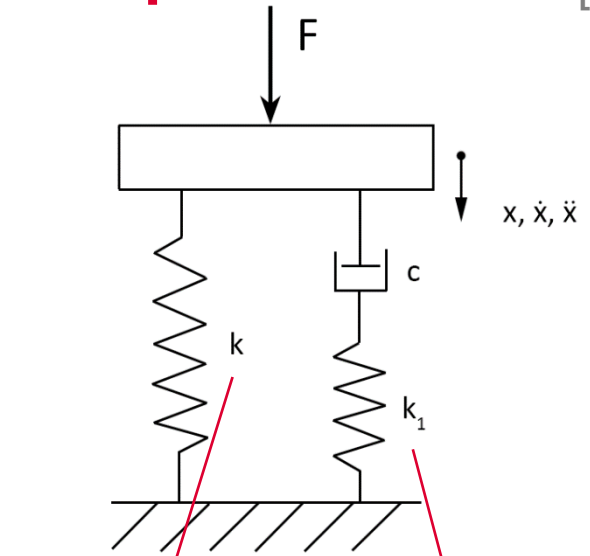
State of art

Elastically connected damper

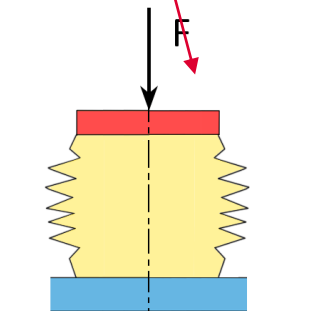
[Harris, 2002]



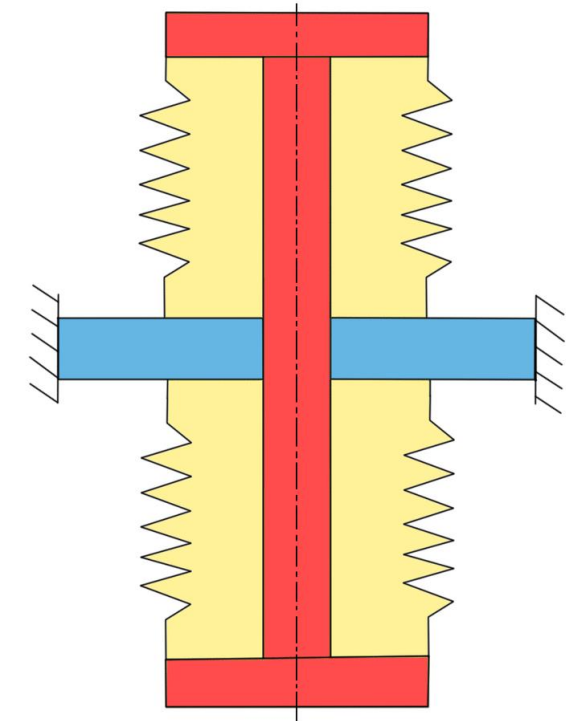
Low damping



Available



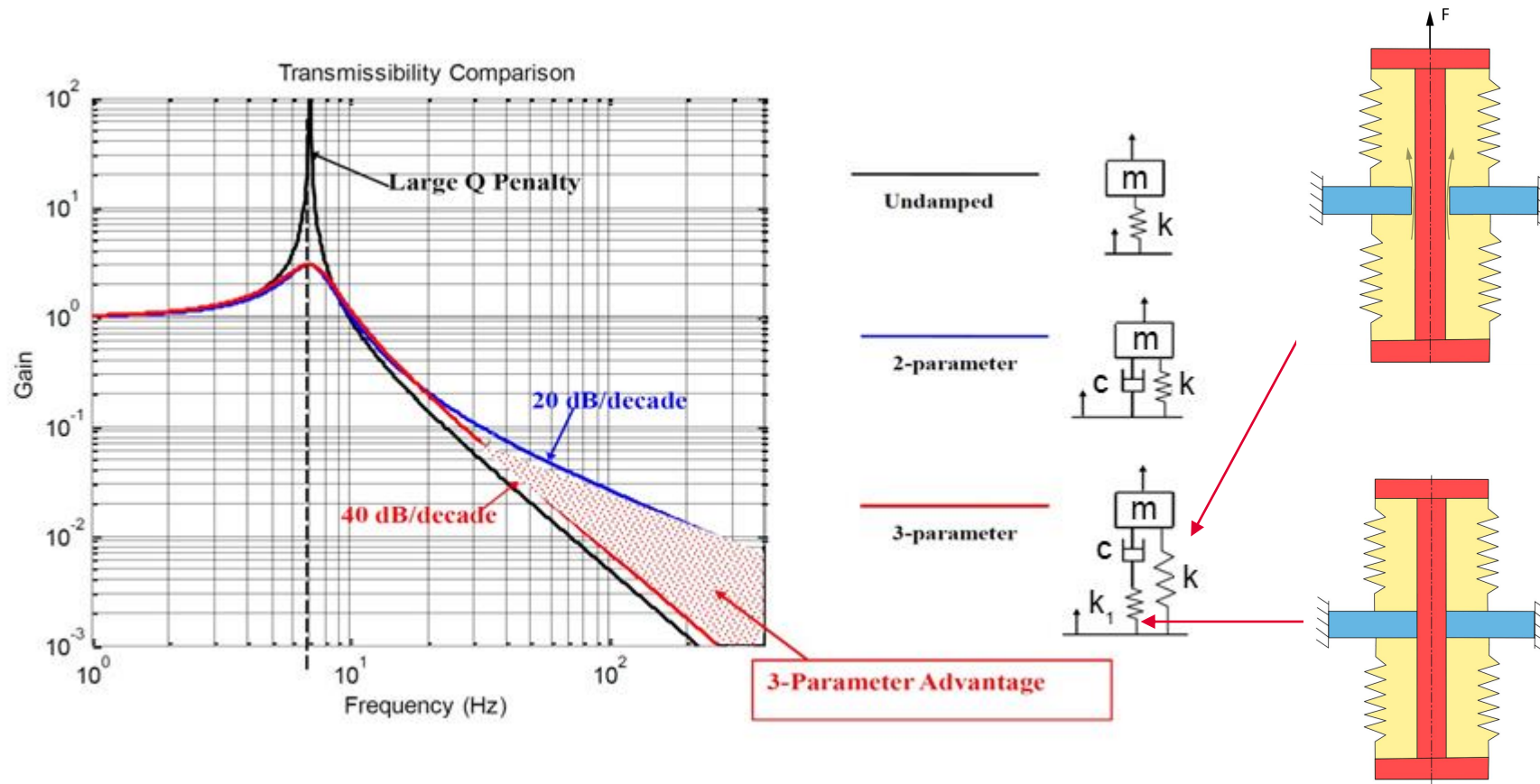
Unavailable



High damping

State of art

Elastically connected damper

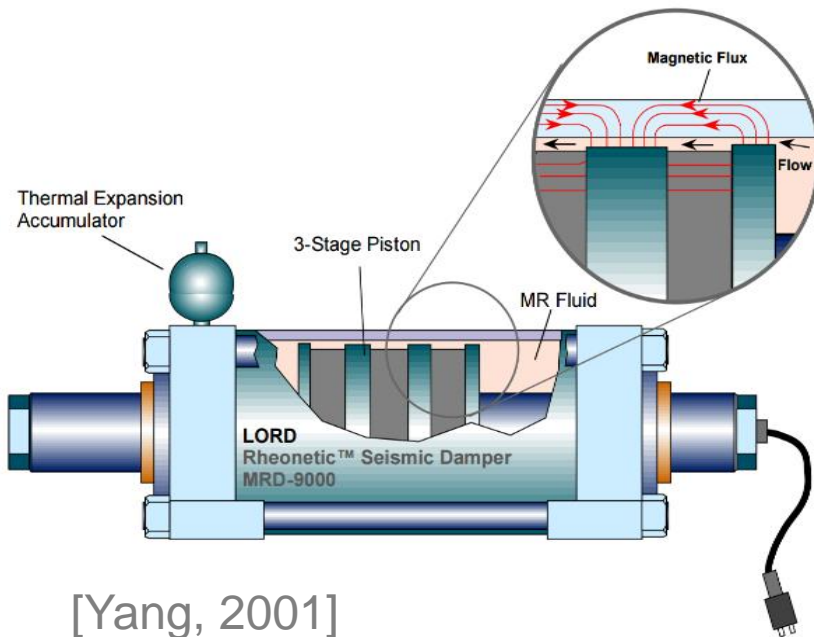


State of art

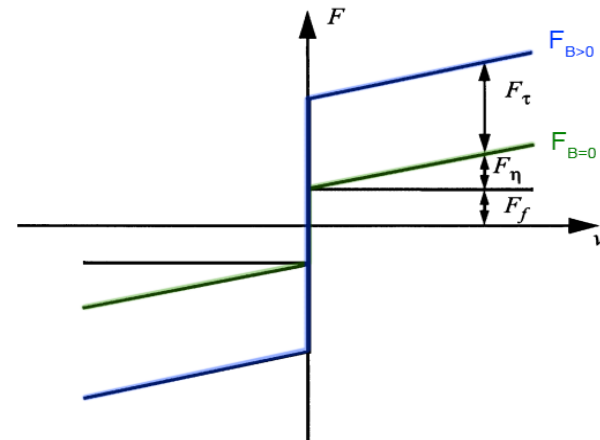
Magnetorheological damper (MR)

Controllable damping force

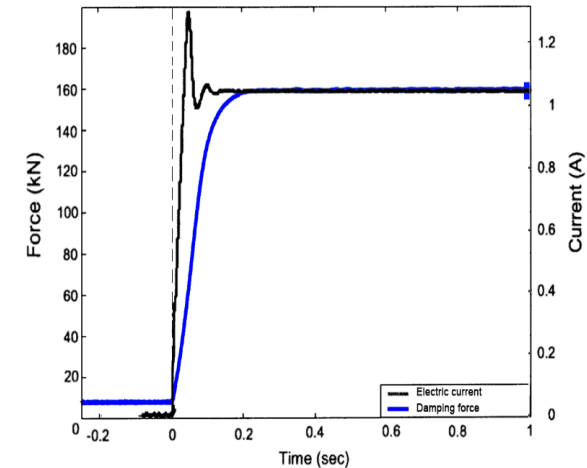
Effective semi-active control \longrightarrow high **Dynamic force range** & **low response time**

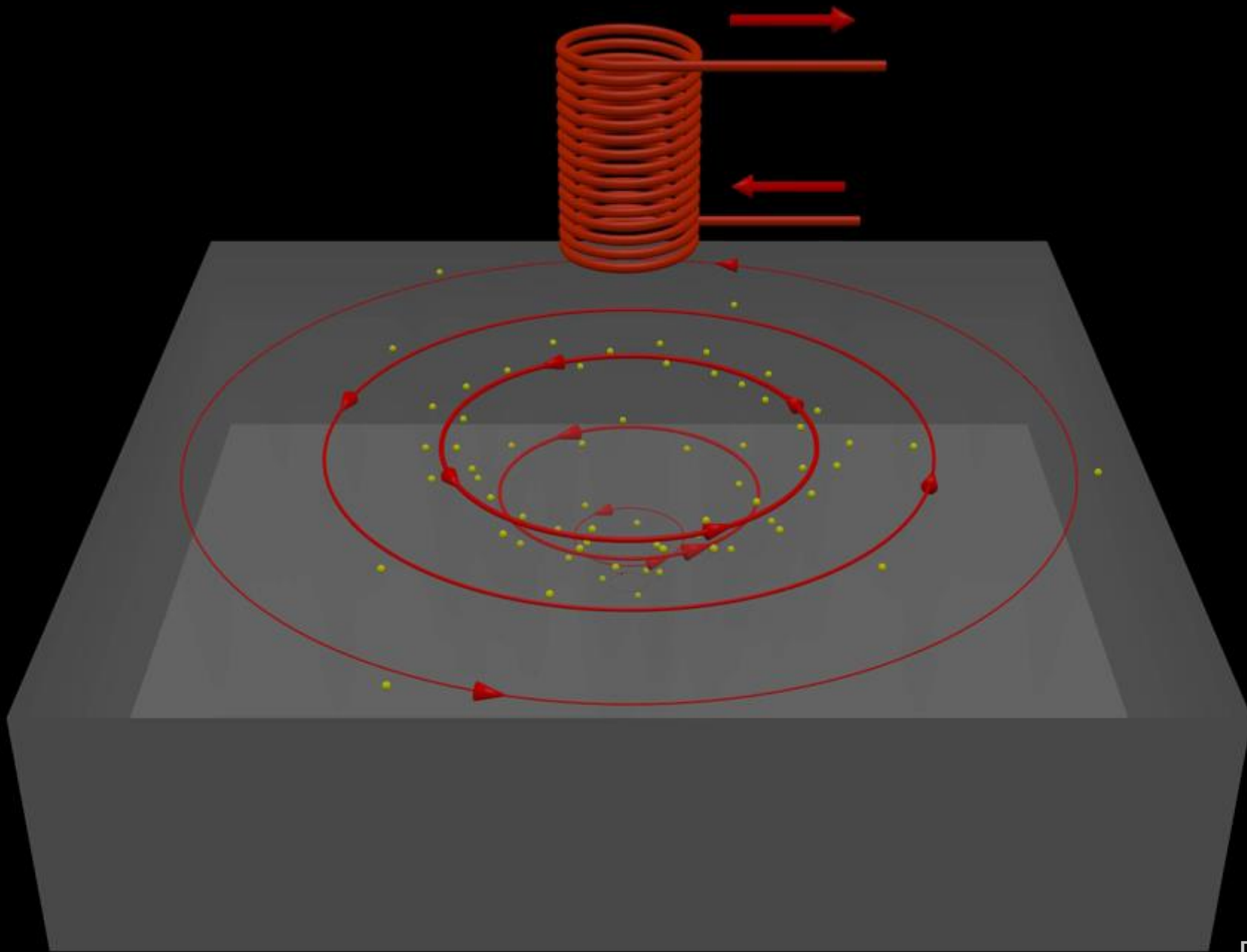


[Yang, 2001]



$$D(v, B) = \frac{F_{B=max}}{F_{B=0}}$$

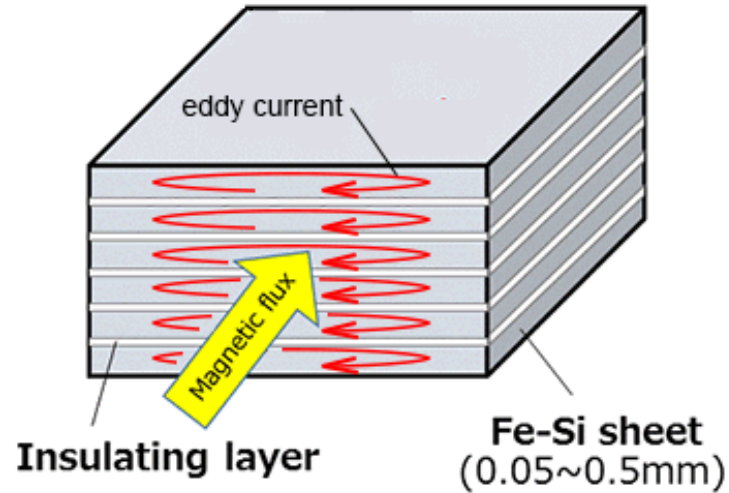




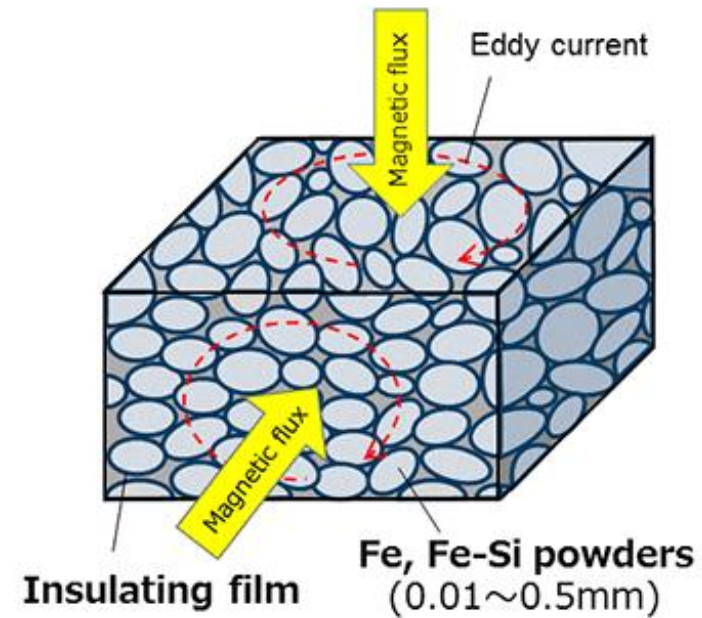
State of art

Eddy current elimination

Shape approach



Material approach

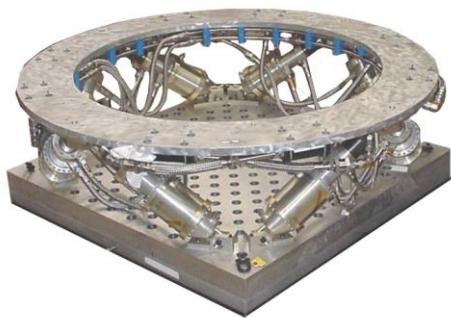


[www.global-sei.com]

Summary of literature review

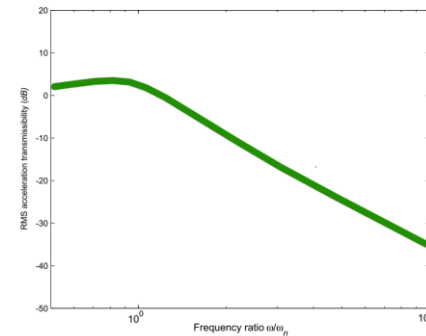
Type of VIS

- Structural
- Based on struts



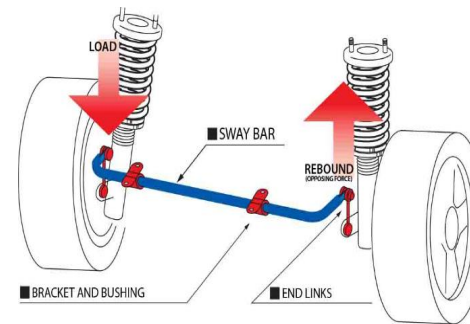
Control strategy

- Passive
- Active
- Semi-active (MR damper)



Stabilizer

- Hydraulic
- Mechanical



Sealing

- Sealing cuff
- Metal bellows

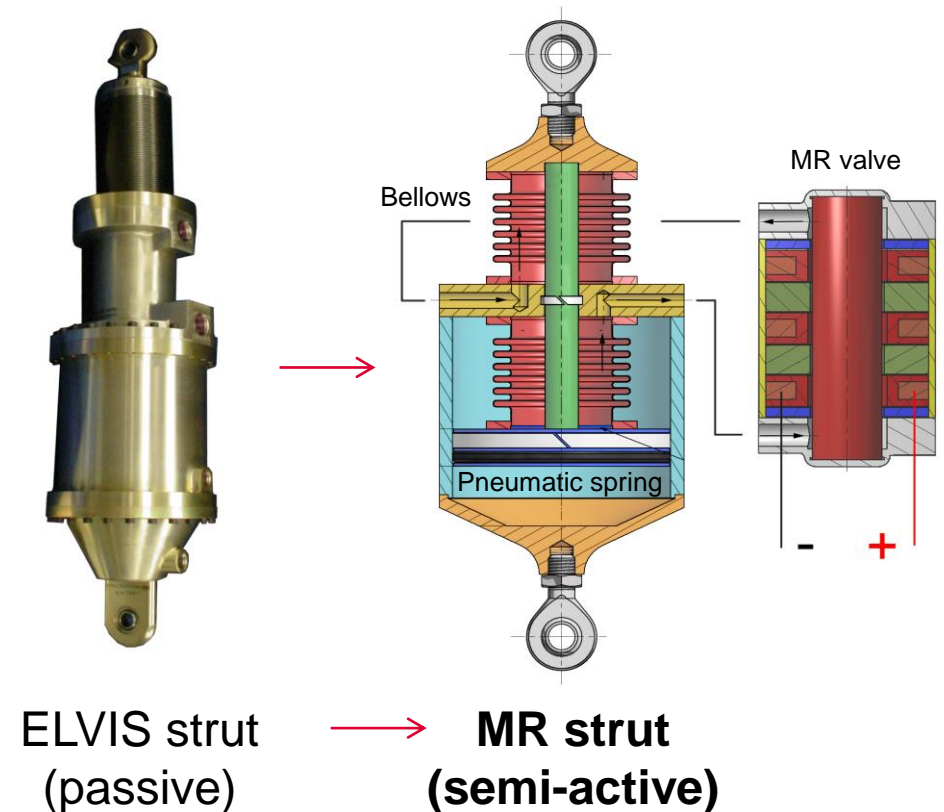


Aim of the thesis

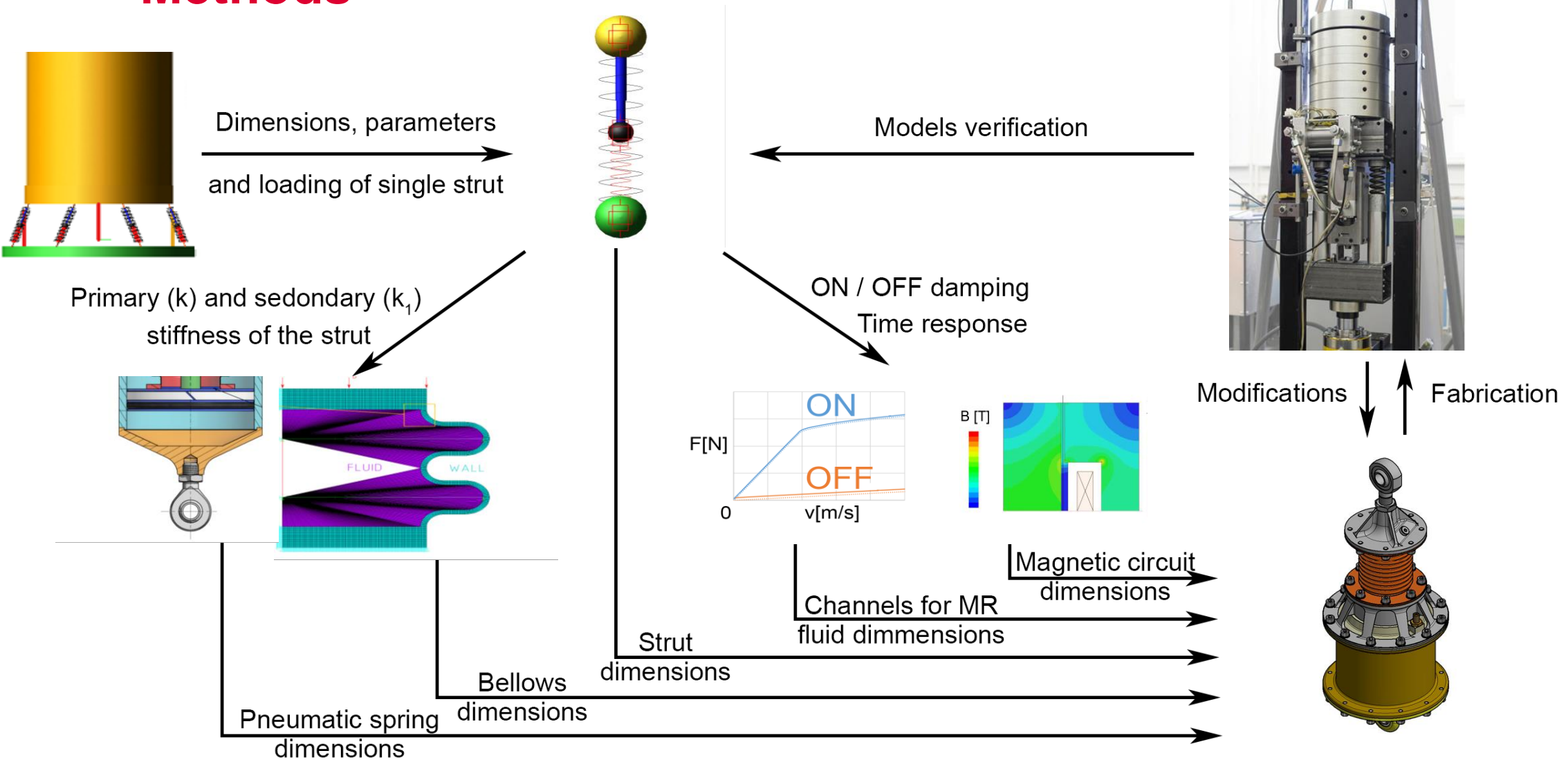
Design of semi-active strut combining spring and damper function for the vibration isolation system of the launch vehicle

Sub aims:

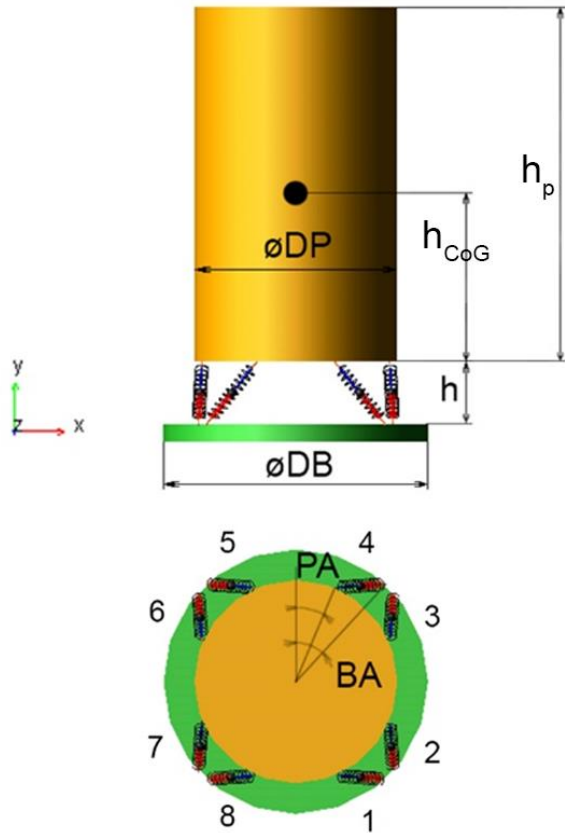
- VIS concept selection
- Determination of single strut load (multibody model)
- Find an optimal parameters of MR damper
- Design dimensions of struts (several models)
- Experimental strut design
- Tests (the models verification)



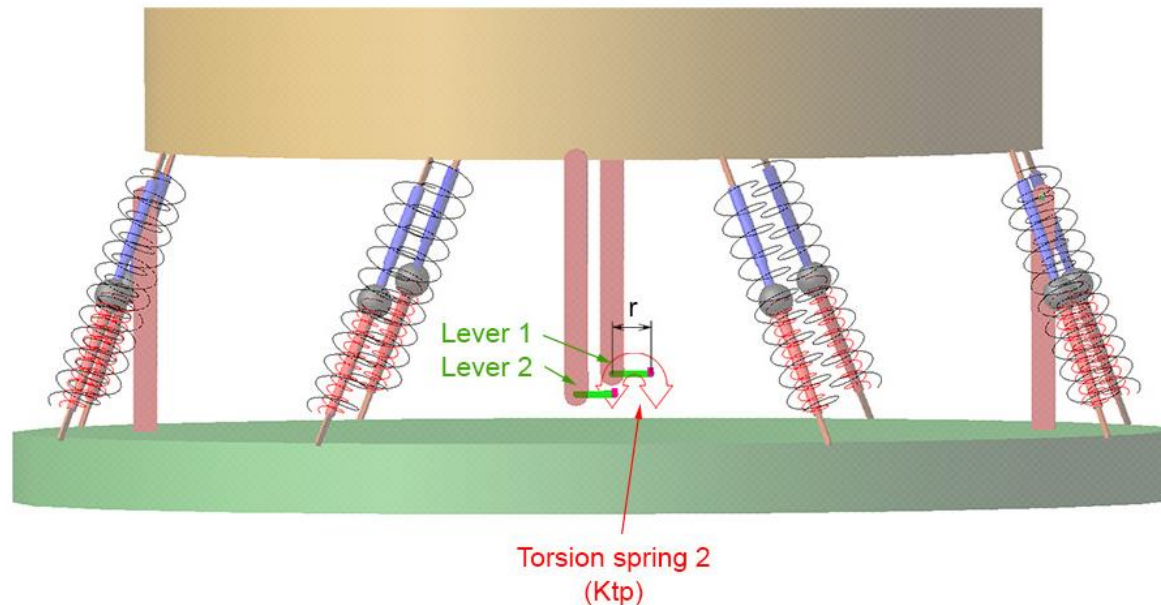
Methods



Dynamic model of VIS

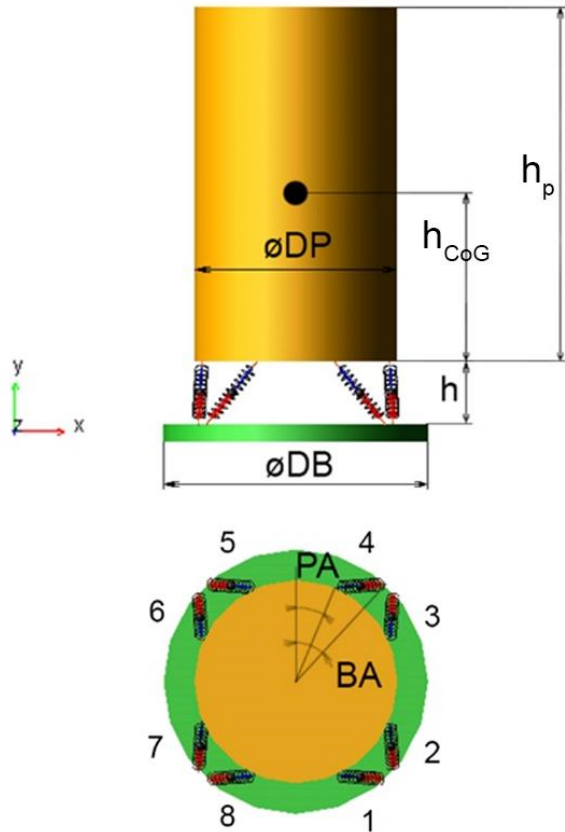


VIS requirements			
Parameter	Symbol	Value	Unit
VIS connection diameter	ϕDB	1920	[mm]
VIS minimum height	h	380	[mm]
Payload connection diameter	ϕDP	1280	[mm]
Payload mass	m	1500	[kg]
Payload centre of mass height	hCoG	1500	[mm]
Max. acceleration (lateral)	a_x	± 0.9	[g]
Max. acceleration (axial)	a_y	± 5.5	[g]
Max. displacement of payload (lateral)	d_x	30	[mm]
Max. displacement of payload (axial)	d_y	10	[mm]

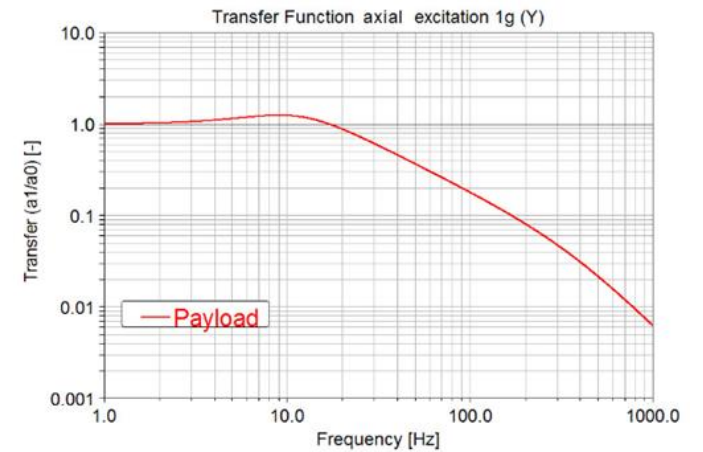
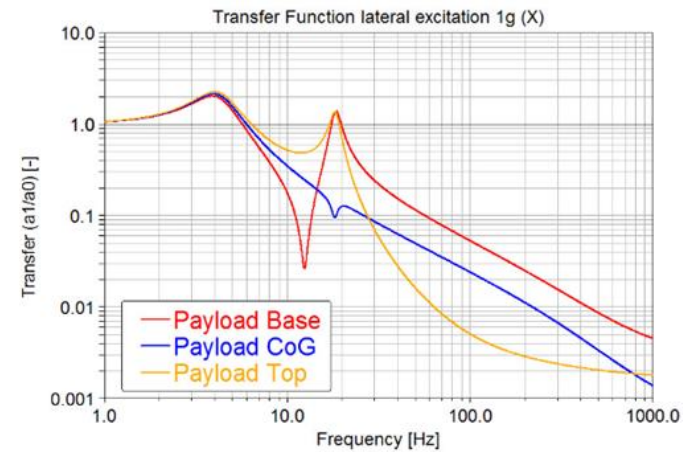


Dynamic model of VIS

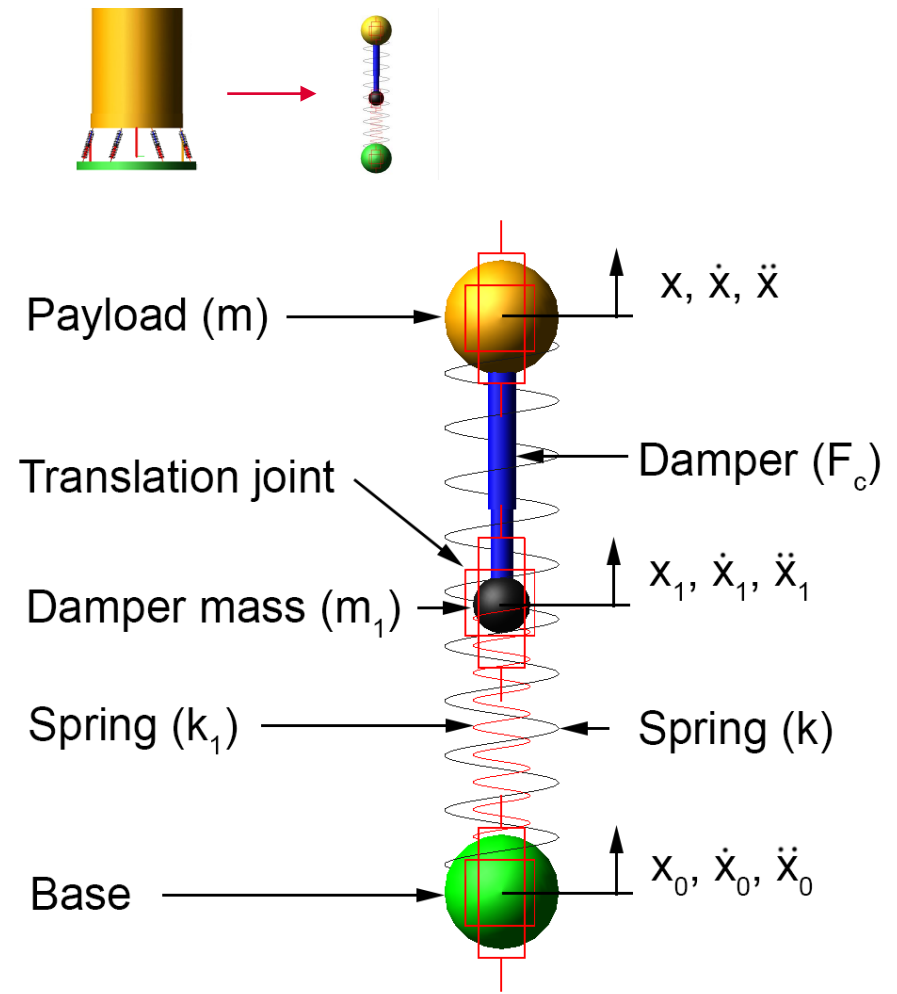
Final configuration



Parameter	Symbol	Value	Unit
Primary stiffness of the strut	k_A	1230	[N/mm]
Damping of the strut	c_A	26	[Ns/mm]
Ratio k_B/k_A	N	50	[-]
Torsion stiffness of stabilizer	k_{MS}	$1.072 \cdot 10^7$	[Nm/rad]
Angle between struts along payload diameter	PA	19	[deg]
Angle between struts along base diameter	BA	26	[deg]
VIS height	h	380	[mm]



Dynamic model of single strut



Parameter	Symbol	Value	Unit
Experimental payload mass	m	100	[kg]
Primary stiffness of experimental strut	k	380	[N/mm]
Damping of the strut (activated state)	C_{ON}	12.5	[Ns/mm]
Time response of the damper	t	?	[ms]
Dynamic force range of the damper ($D = C_{ON}/C_{OFF}$)	D	?	[-]
Secondary stiffness of experimental strut	k_1	?	[N/mm]

Semi-active control
(ON/OFF skyhook)

$$\dot{x} \cdot (\dot{x} - \dot{x}_1) \geq 0 \rightarrow F_c = F_{cmax}$$

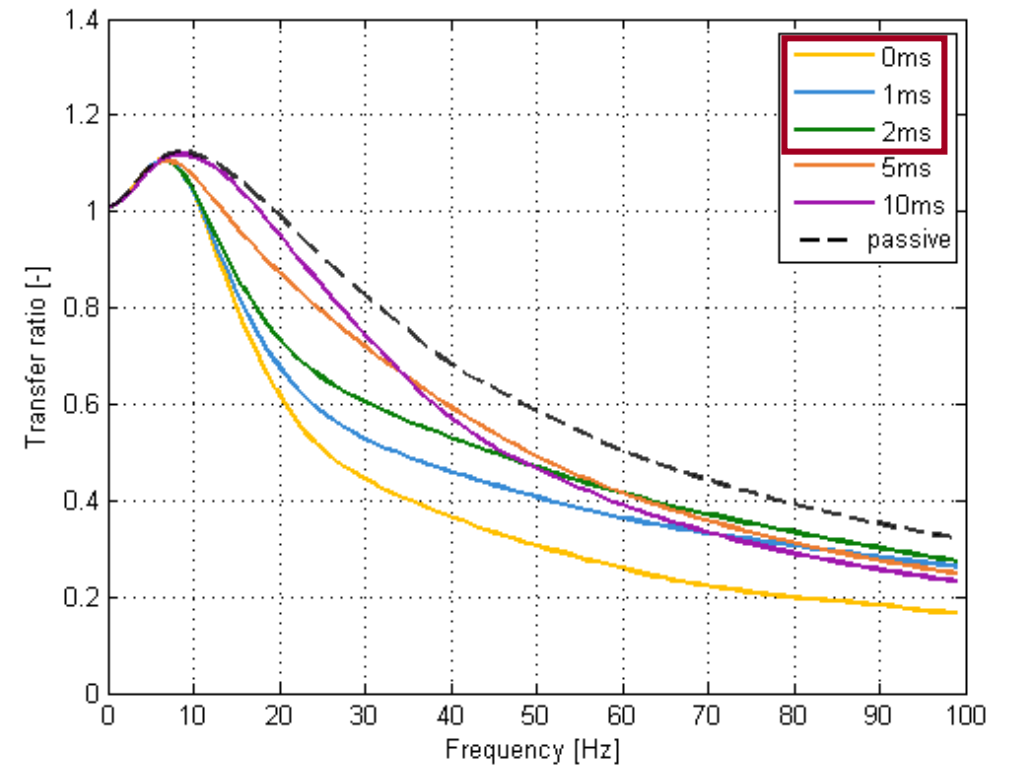
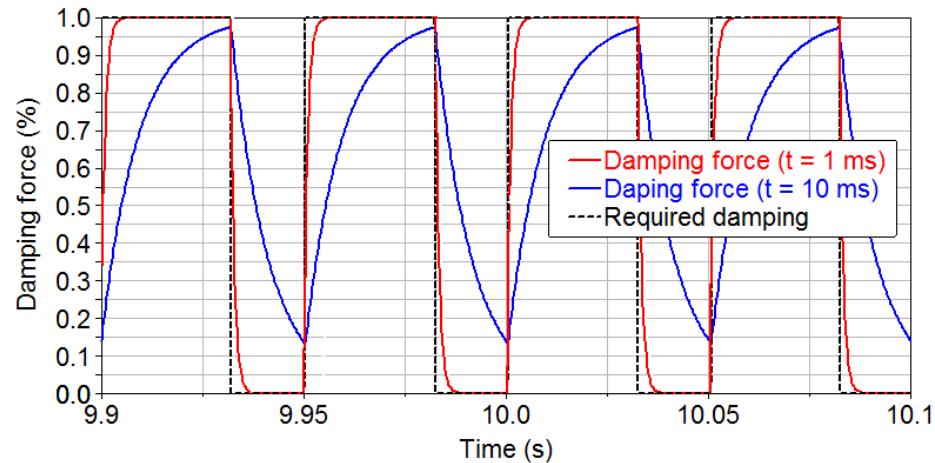
$$\dot{x} \cdot (\dot{x} - \dot{x}_1) < 0 \rightarrow F_c = F_{cmin}$$

Dynamic model of single strut

Semi – active control

Influence of MR damper time response

Force comparison of **fast** and **slow** damper

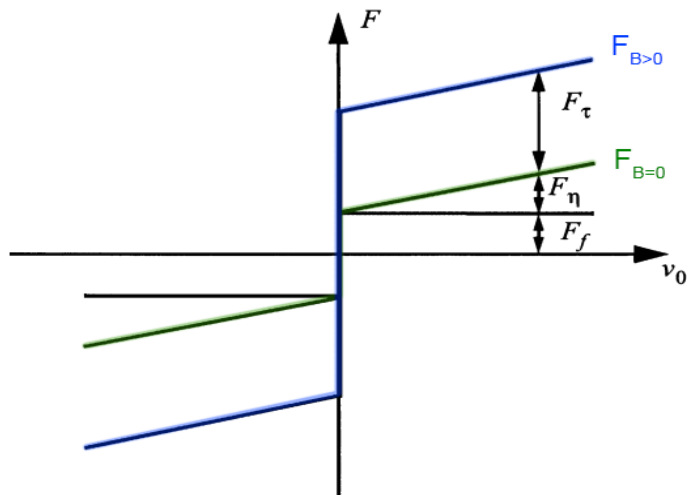


Dynamic model of single strut

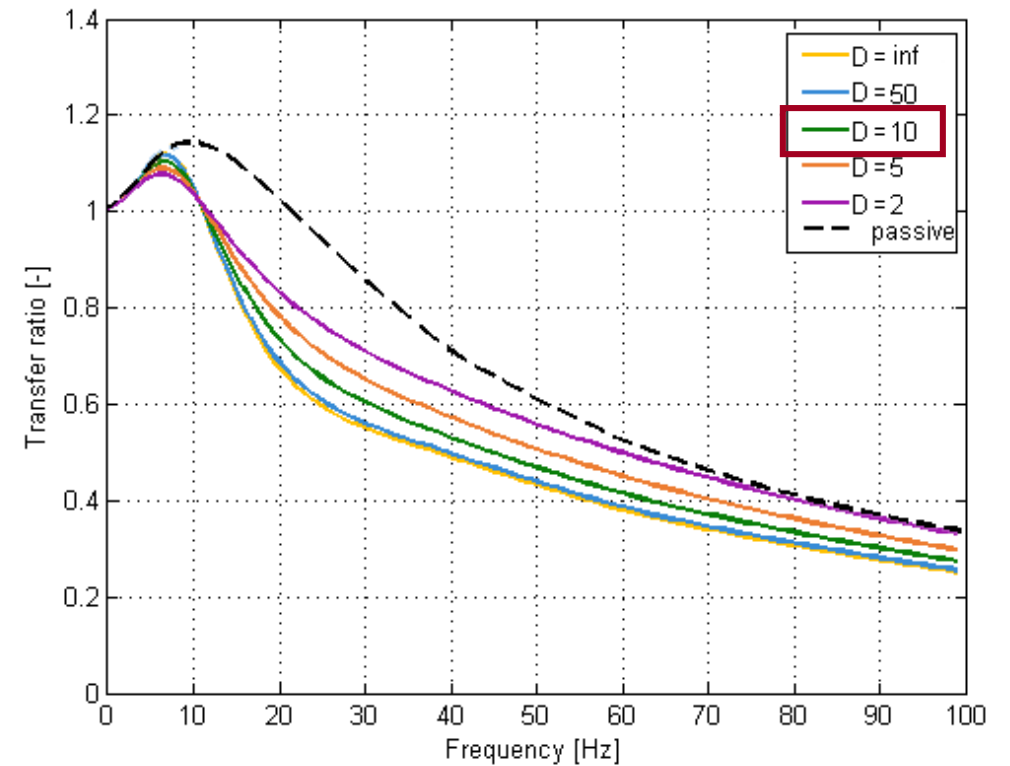
Semi – active control

Influence of MR damper dynamic force range

Typical F-v dependency of MR damper



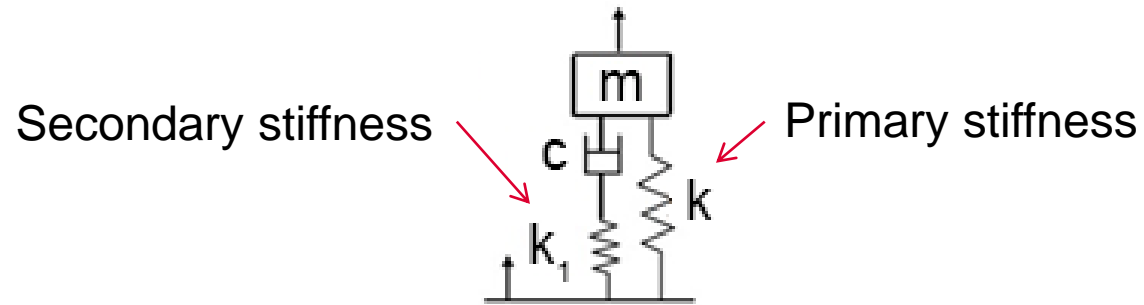
$$D(v, B) = \frac{F_{B=max}}{F_{B=0}}$$



Dynamic model of single strut

Semi – active control

Influence of MR damper secondary stiffness (k_1)

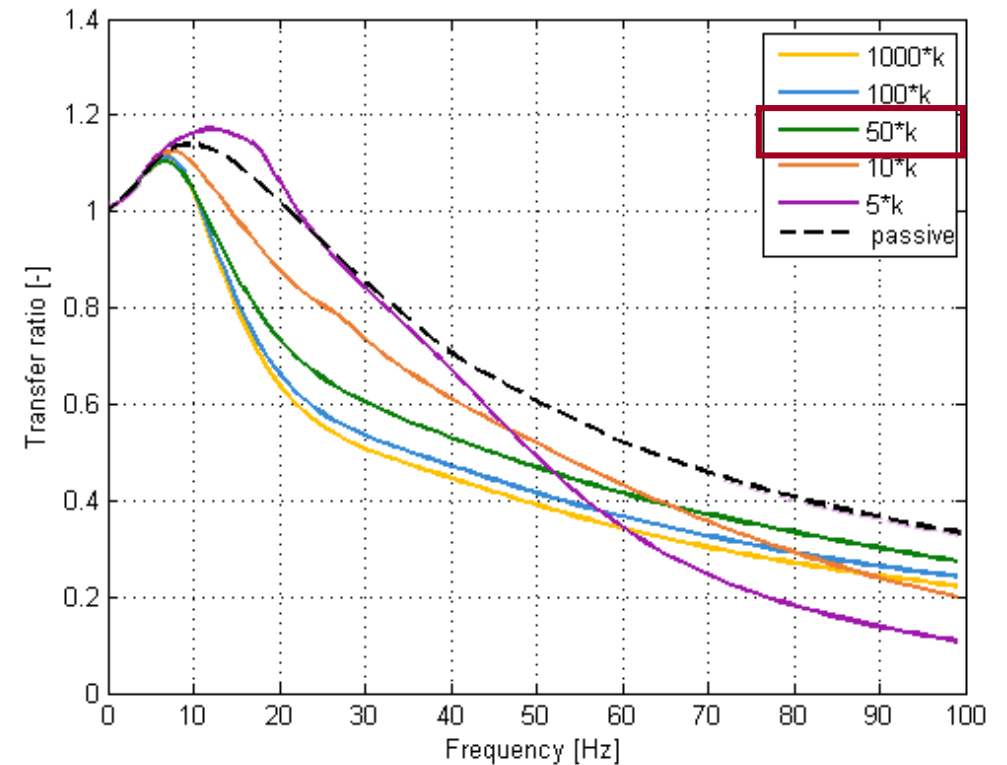


Conclusion of simulations:

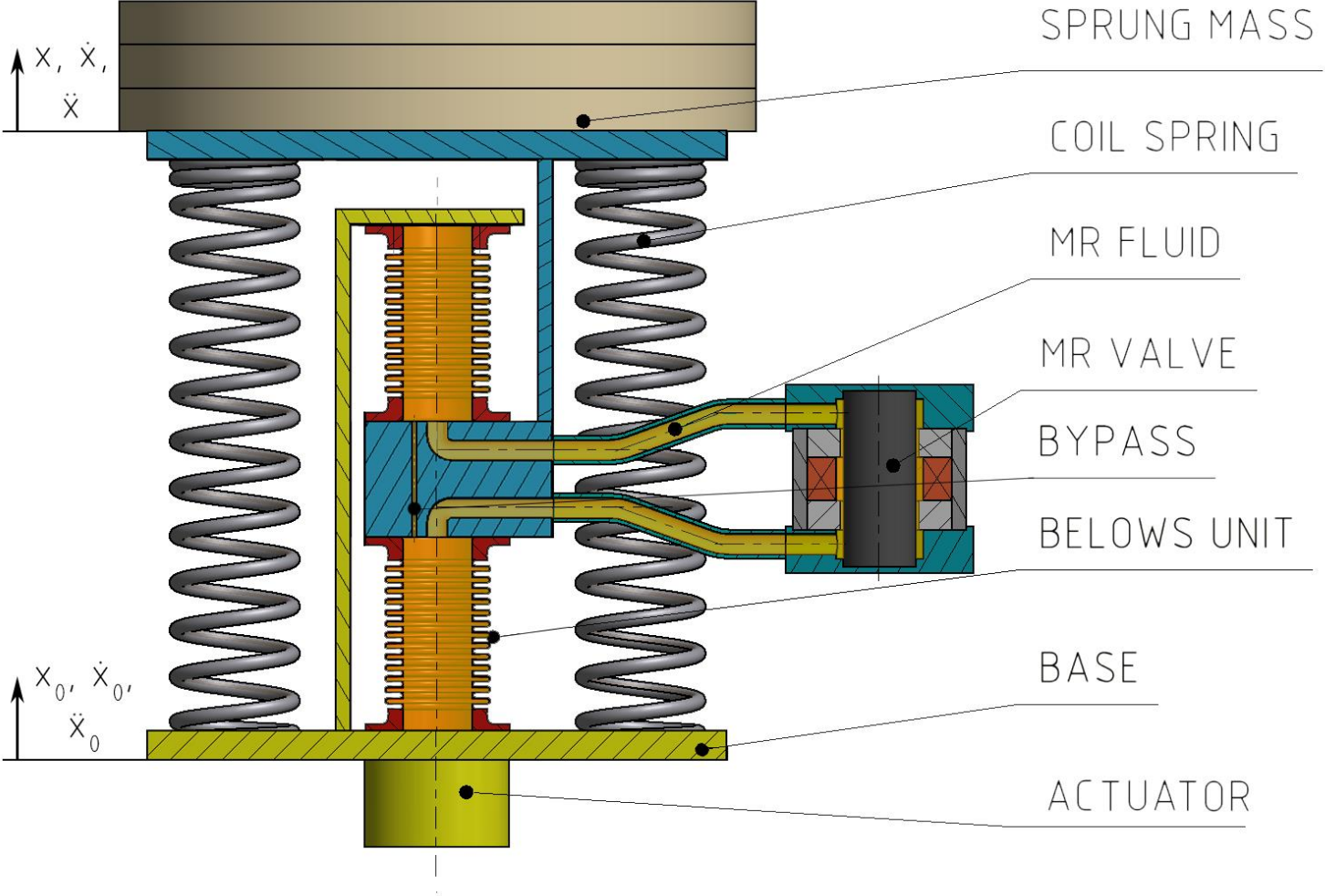
Time response: < 2ms

Dynamic force range: approx. 10

Secondary stiffness: $k_1 = \text{approx } 50 \cdot k$

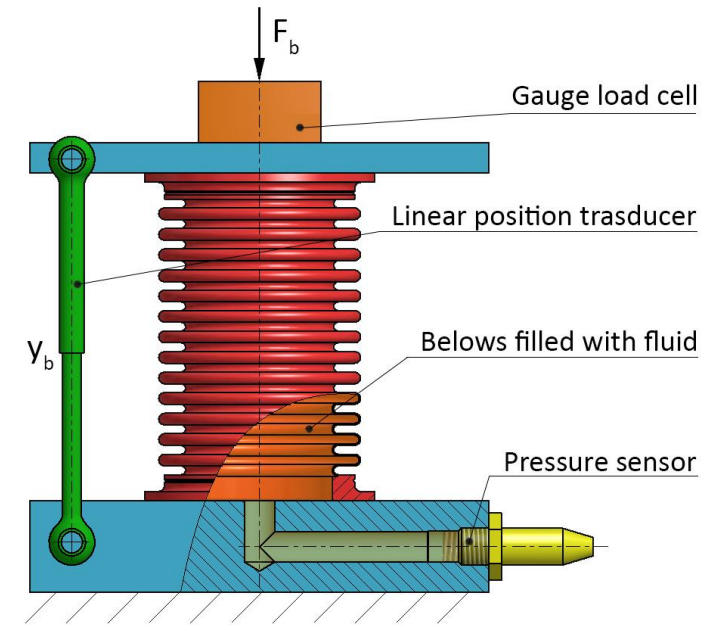
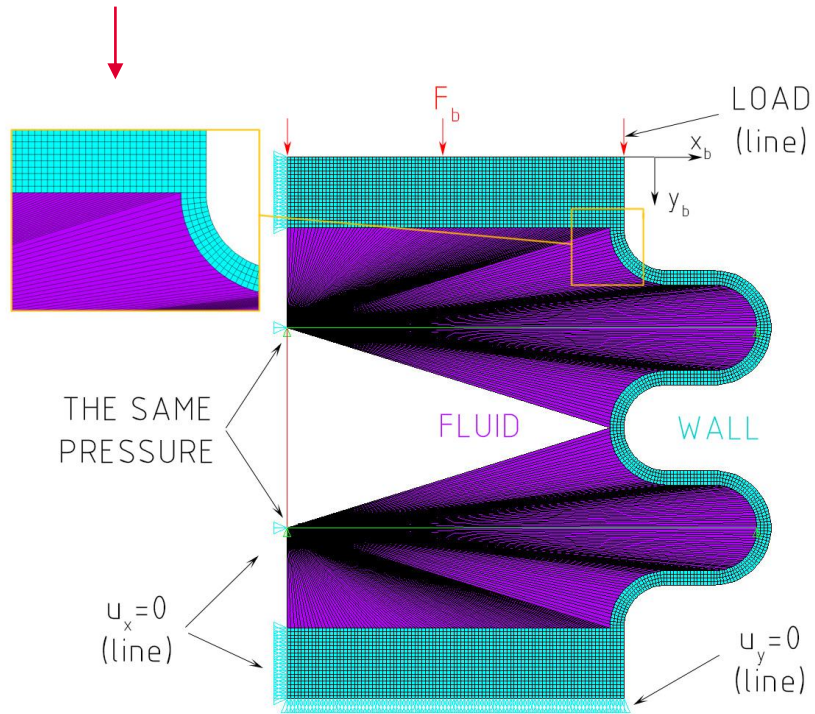


Experimental strut



Metal Bellows

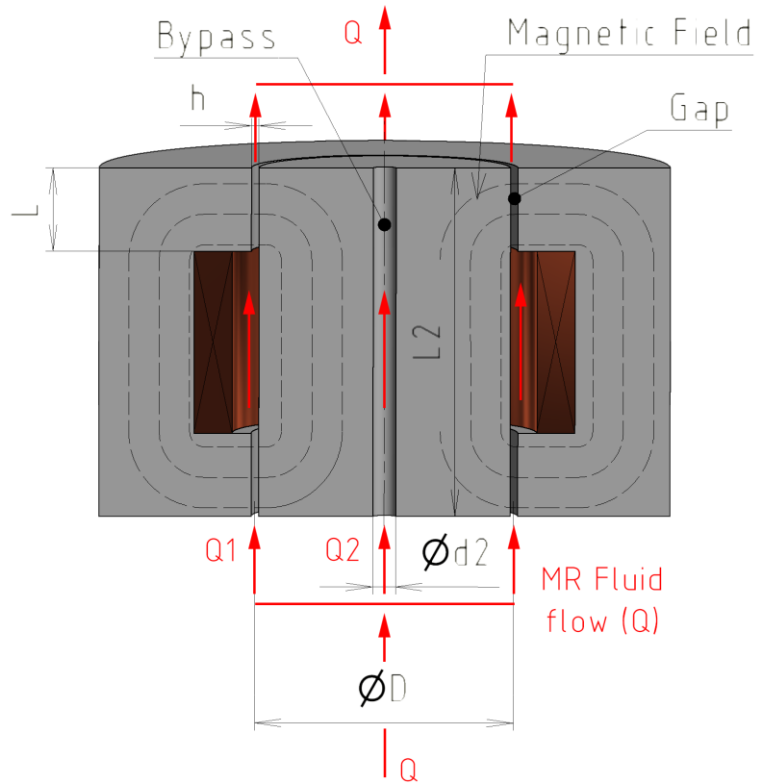
FEA of metal bellows was verified by Measurement



FEA vs simulation: 11 % (axial stiffness); 5.7 % (pressure thrust stiffness)

MR valve design

Hydraulic part

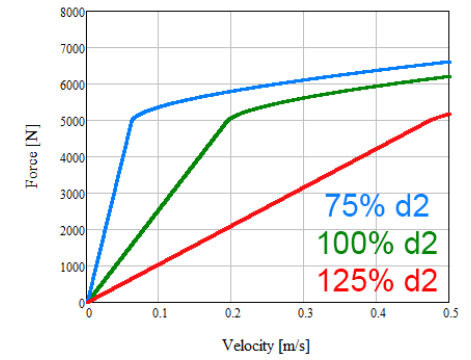
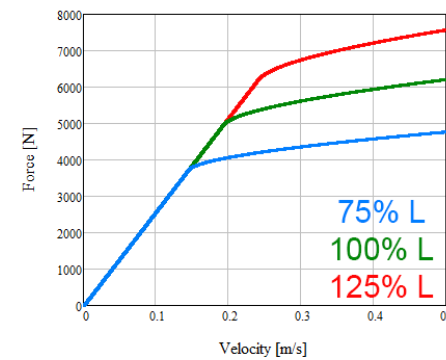
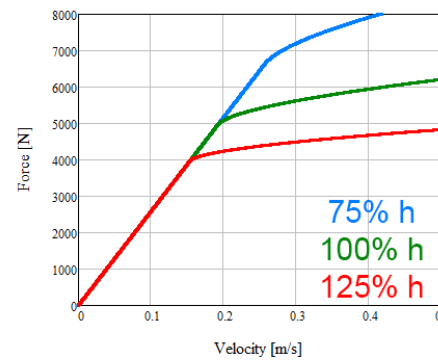


$$F = F_{gap} + F_{bypass}$$

$$F_{gap} = \left(1 + \frac{\pi \cdot D \cdot h \cdot v_0}{2 \cdot Q1} \right) \frac{12 \cdot \eta \cdot Q1 \cdot L \cdot A_p}{\pi \cdot D \cdot h^3} + c \cdot \frac{\tau_0 \cdot L \cdot A_p}{h} \cdot \text{sgn}(v_0)$$

$$F_{bypass} = \left(1 + \frac{\pi \cdot d_2^2 \cdot v_0}{8 \cdot Q1} \right) \frac{48 \cdot \eta \cdot Q2 \cdot L2 \cdot A_p}{\pi \cdot d_2^4}$$

[Yang, 2001]



Measurement of MR valve

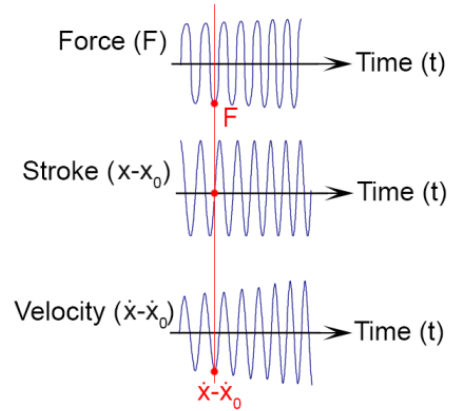
Force – velocity dependency
+
Dynamic range

$$D = 9$$

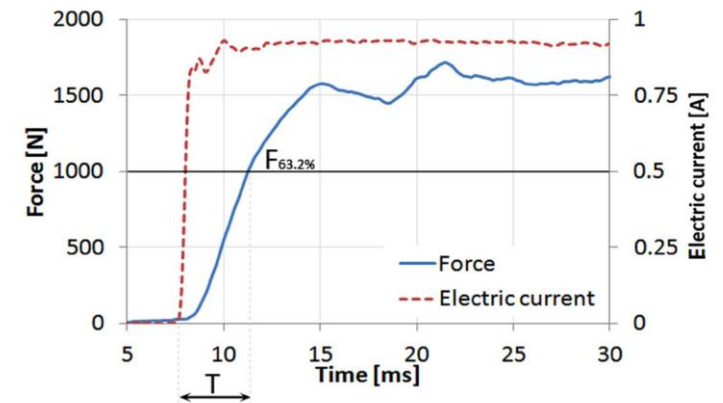
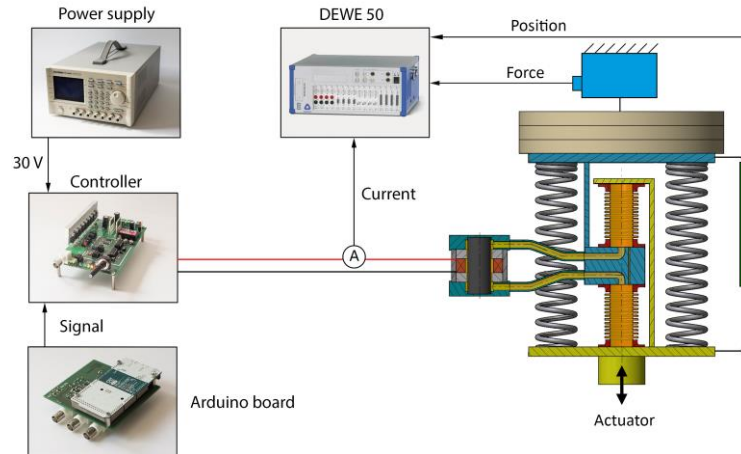
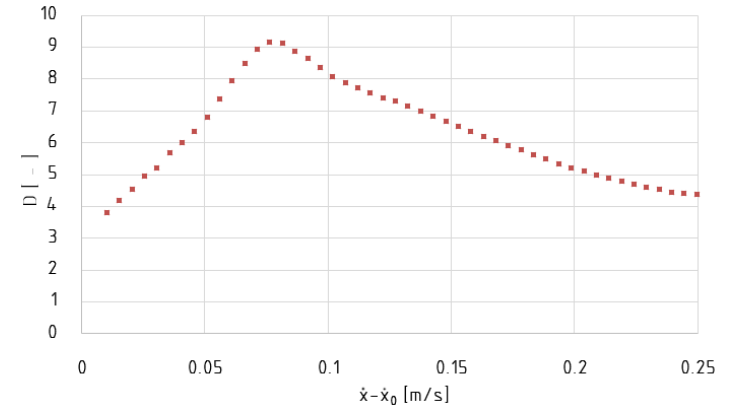
Time response

$$t = 3.9 \text{ ms}$$

Methods



Results



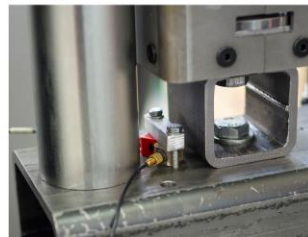
Demonstrator



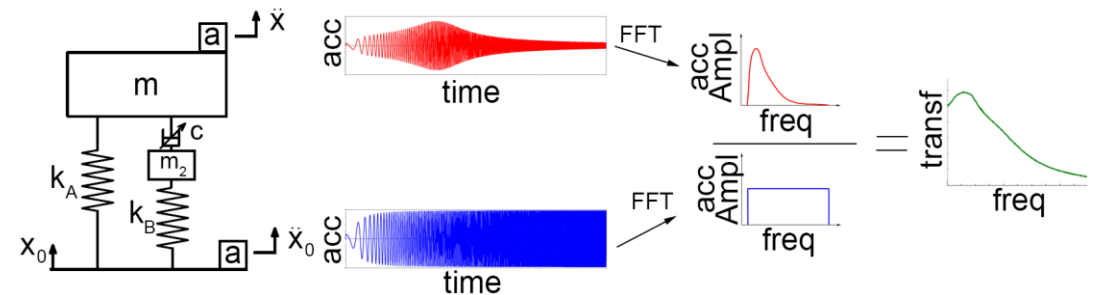
← Payload acceleration (response)



← Relative displacement - > velocity (control)



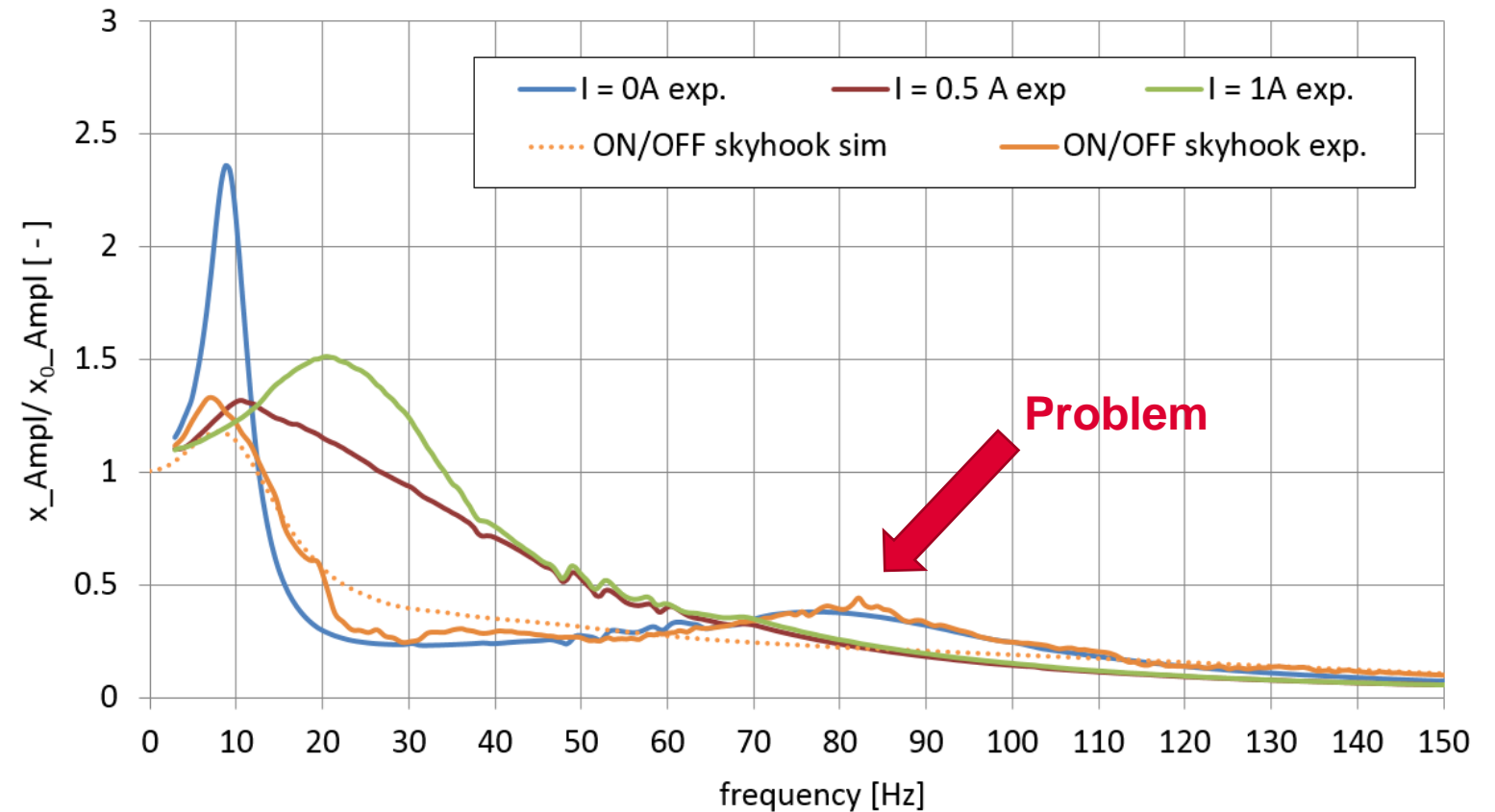
← Base acceleration (excitation)



Measurement results

Transmissibility of experimental MR strut

Semi-active
(ON/OFF skyhook)
 $D = 9$, $t = 4$ ms



Measurement results

Conclusion of measurement of experimental MR strut

Cause of second peak:

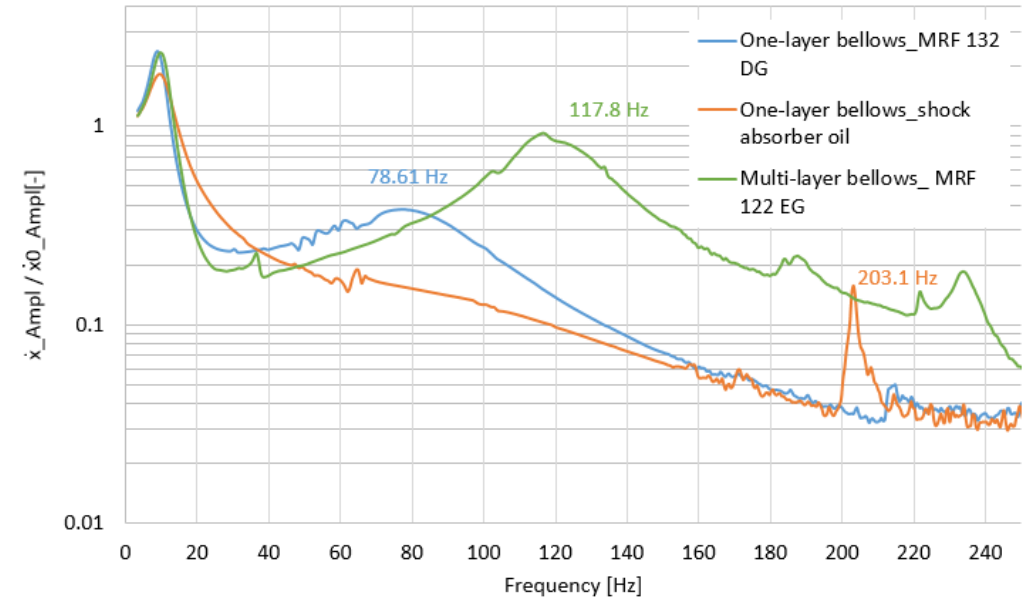
mass effect – fluid mass oscillation in elastic casing

$$f = \frac{\sqrt{\frac{k_t}{m_f}}}{2 \cdot \pi}$$

$$\frac{1}{k_t} = \frac{1}{k} + \frac{1}{k_1}$$

$$m_f = \rho \cdot V$$

Configuration	Counting [Hz]	Measurement [Hz]	Deviation [%]
Multi-layer, MRF 138 EG	146.9	117.8	25
Single-layer, MRF 132 DG	115.2	78.6	47
Single-layer, oil	209.6	203.1	3



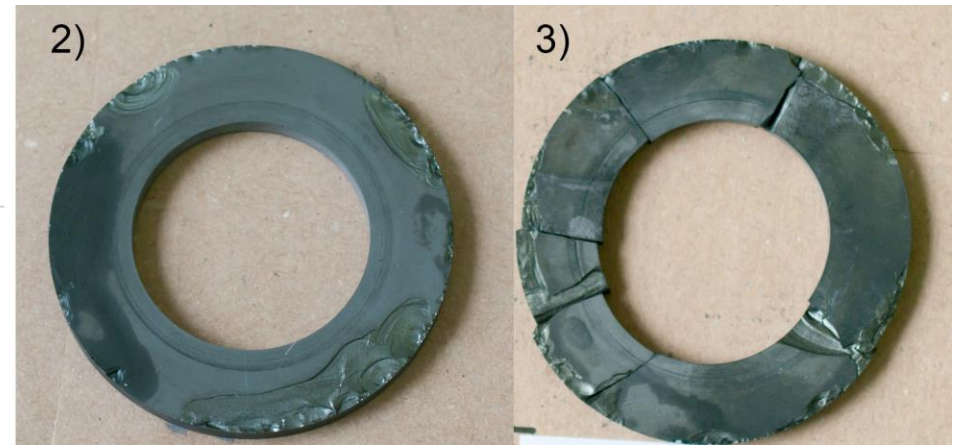
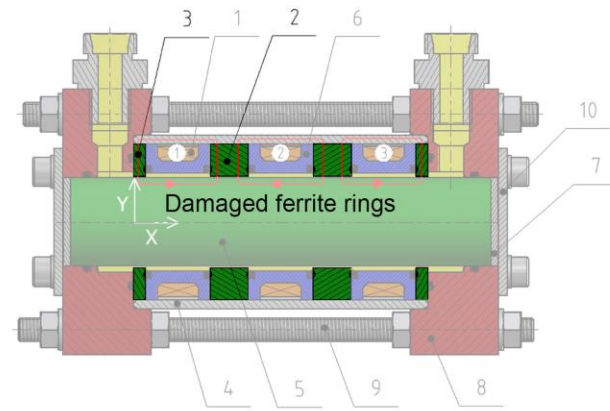
Minimize the fluid mass

Low volume, low concentration of iron

Measurement results

Conclusion of measurement of experimental MR strut

Ferrite rings cracked:

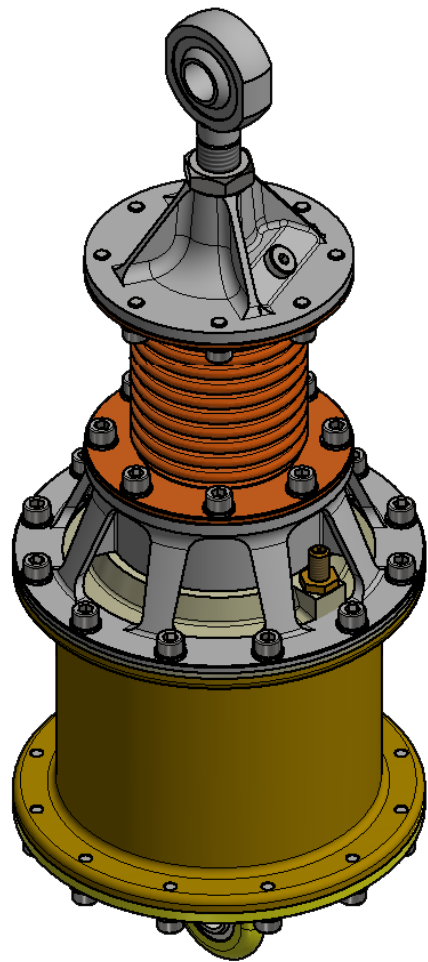


Material approach

↓
Shape approach



Design of MR for VIS of launch vehicle



Damping branch

MR valve

MR Fluid

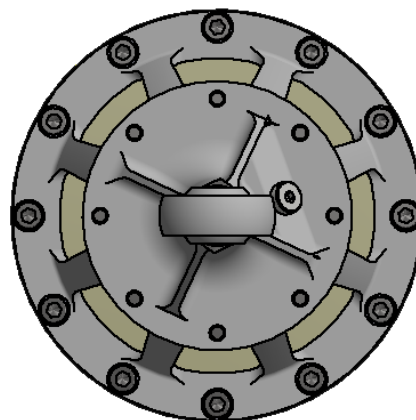
Spring branch

Pneumatic spring,
Bellows

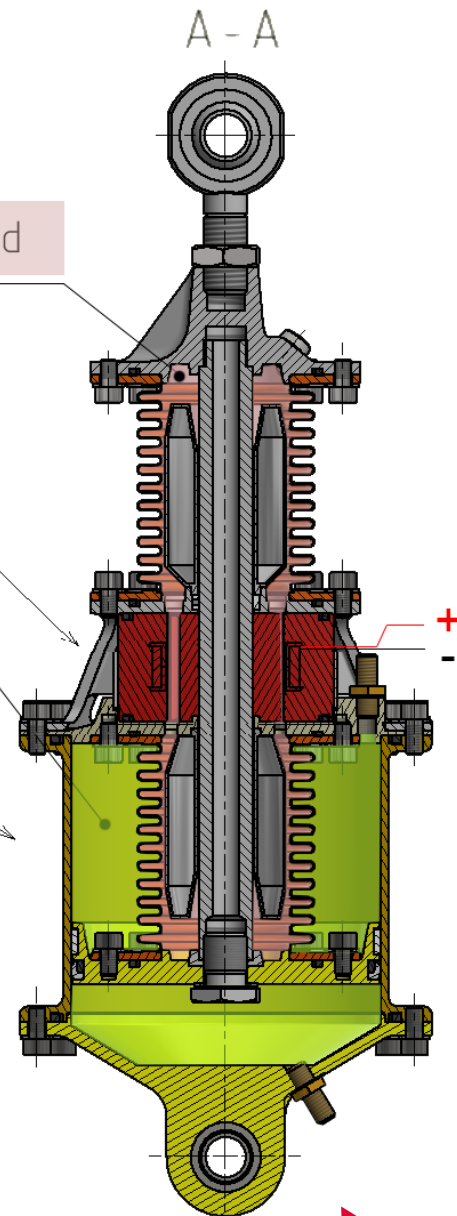
Nitrogen

A - A

A ↑



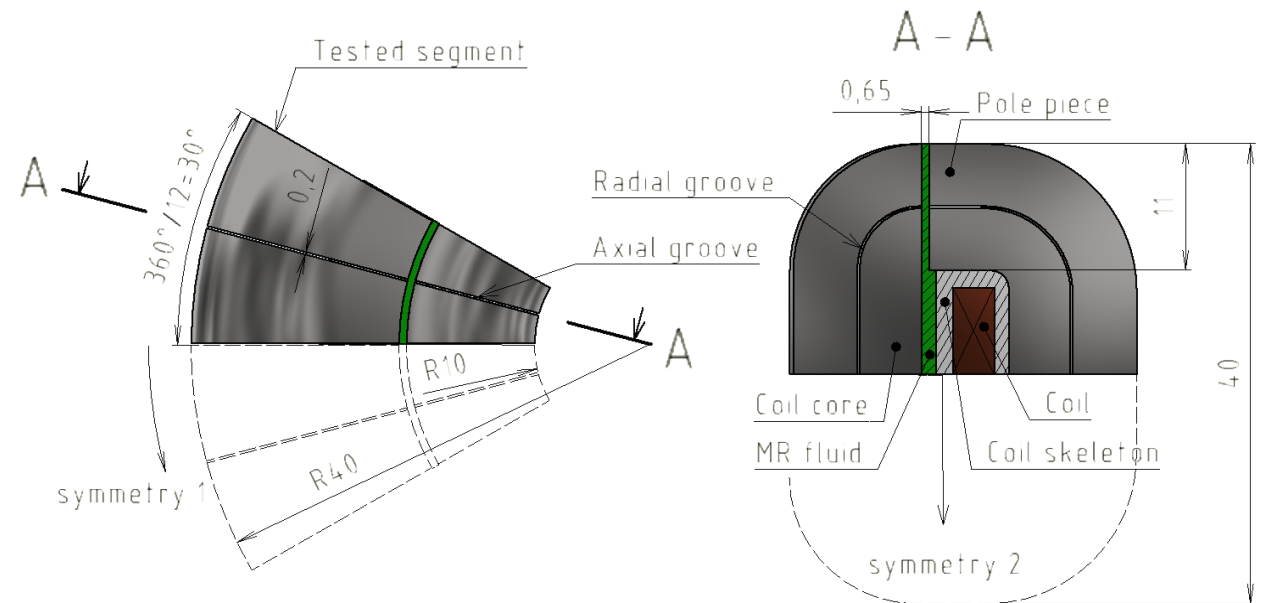
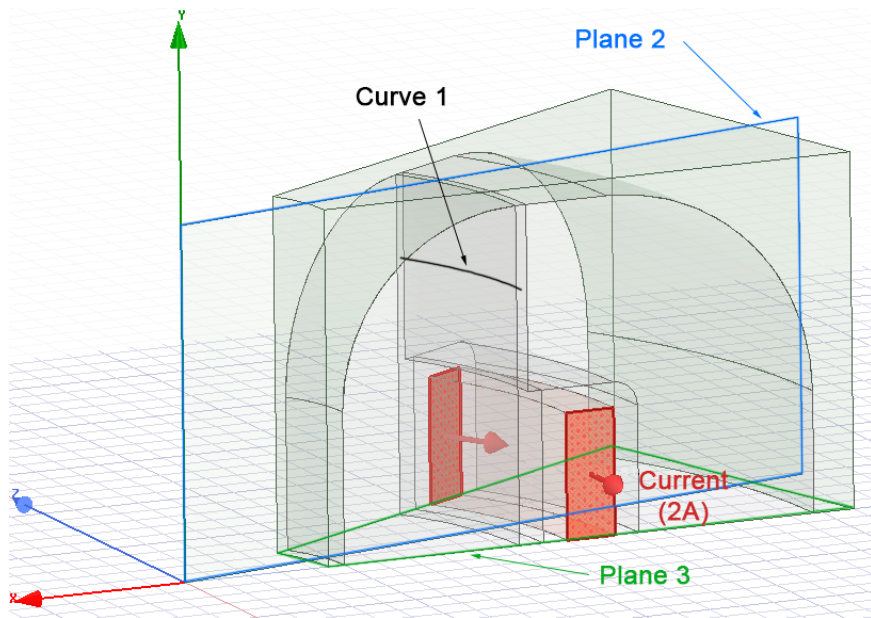
↑ A



MR valve design

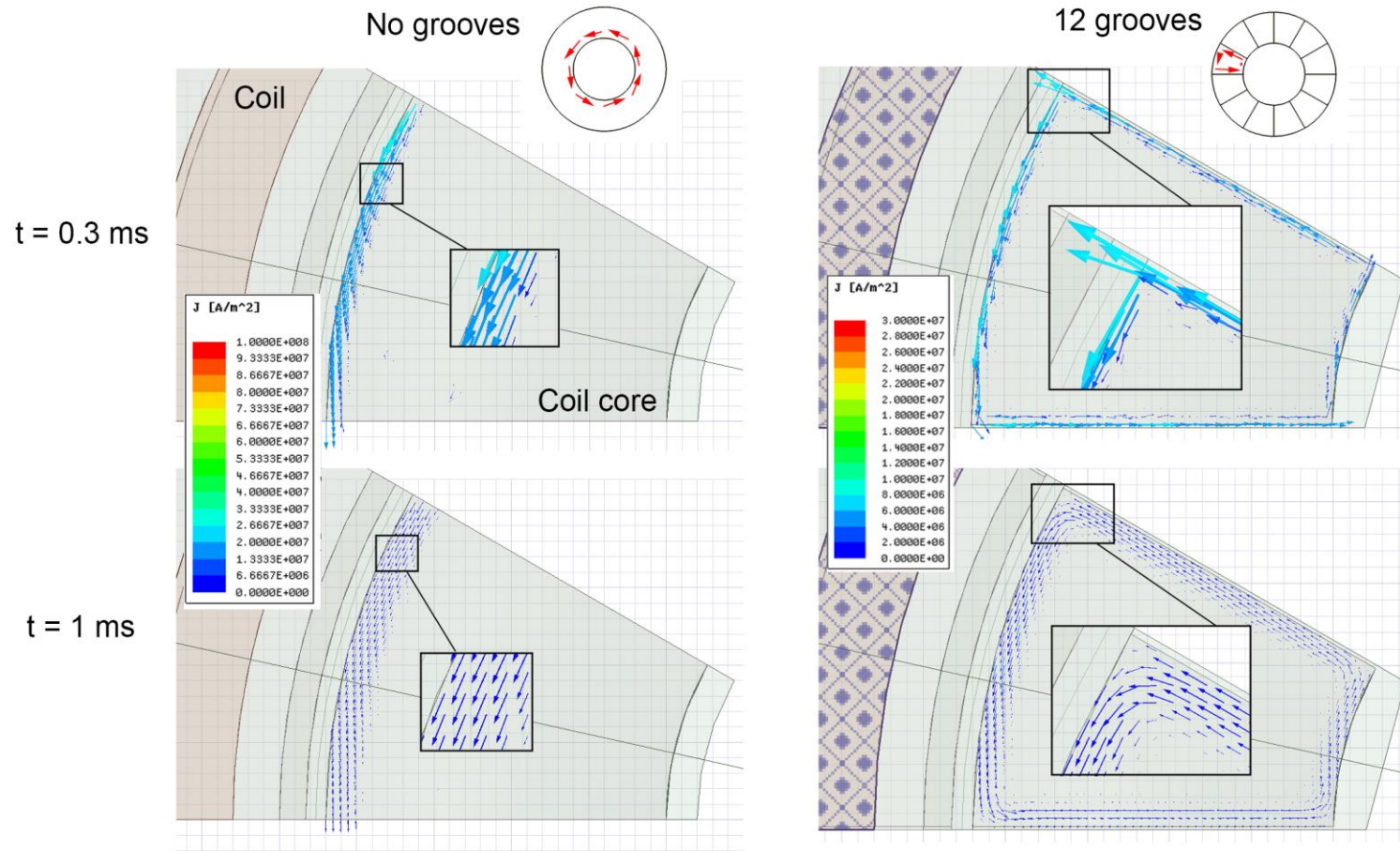
Magnetic part

Goal – Minimize eddy current to achieve fast time response of MR valve



MR valve design

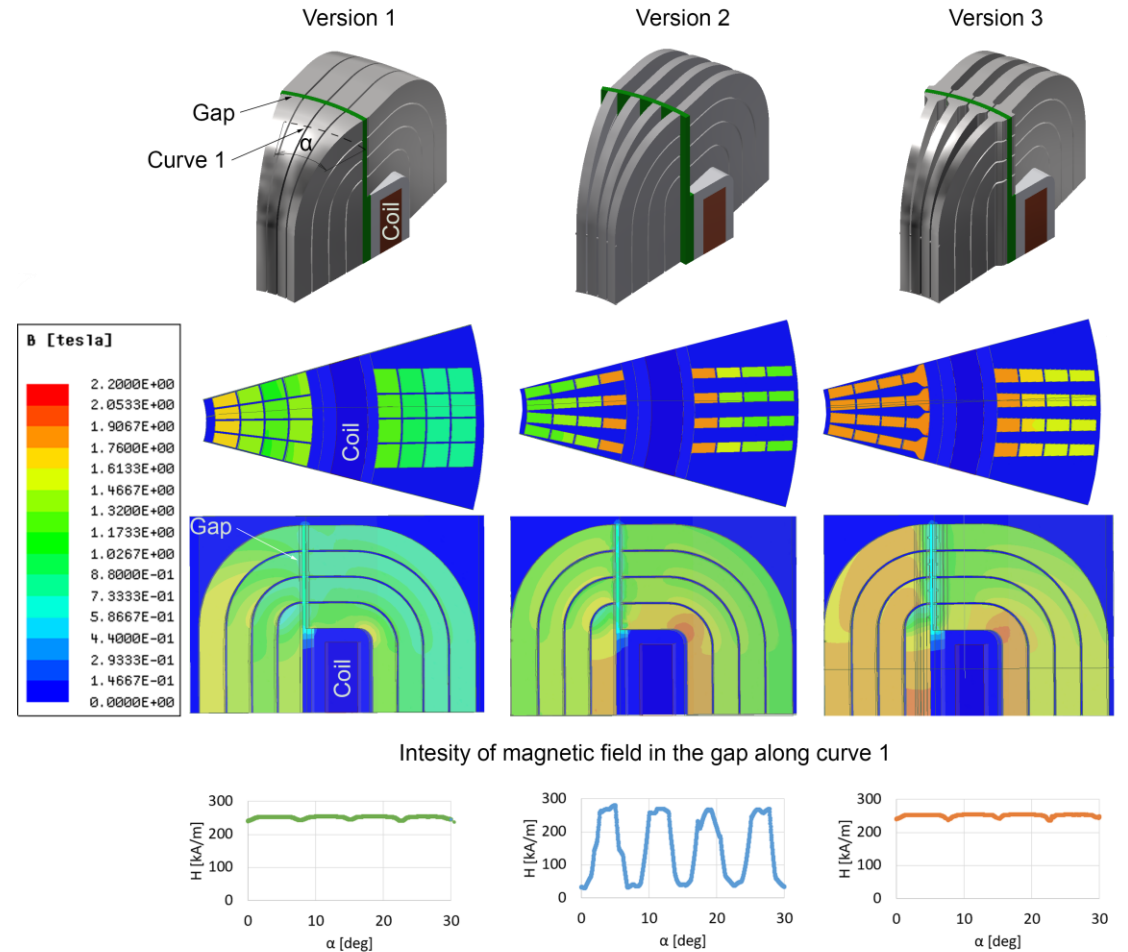
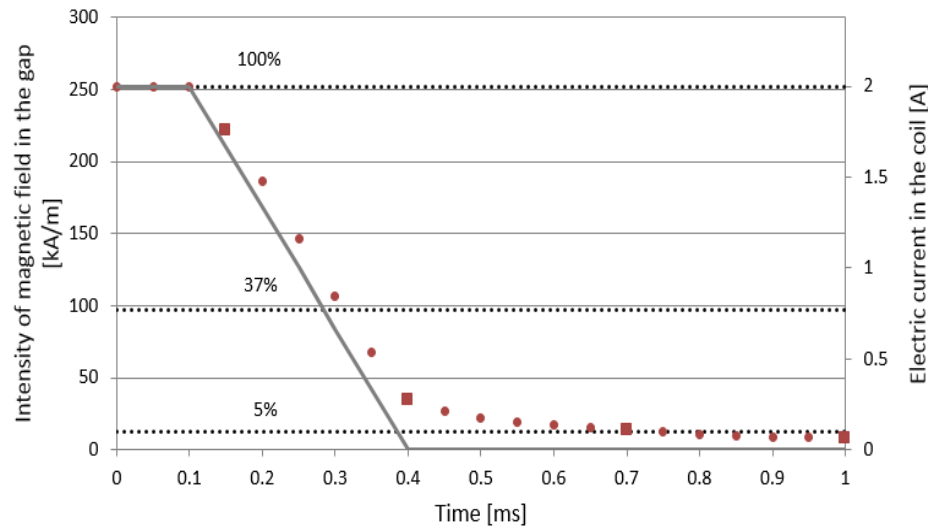
Eddy current in the magnetic circuit



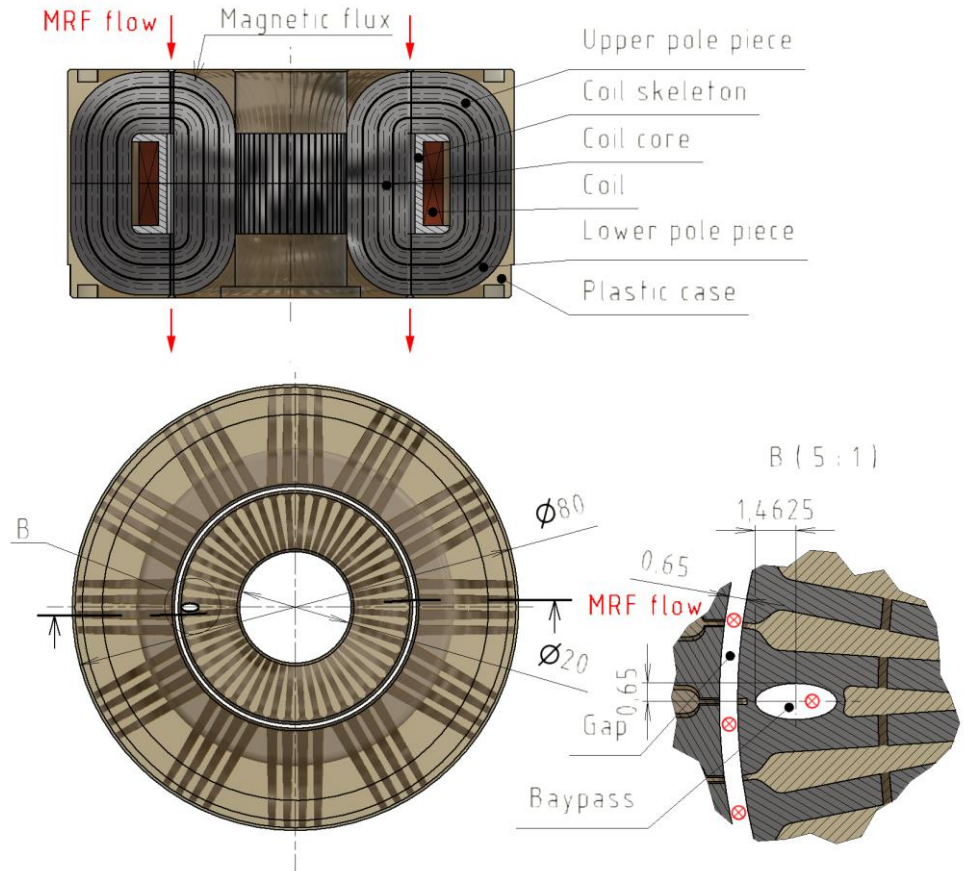
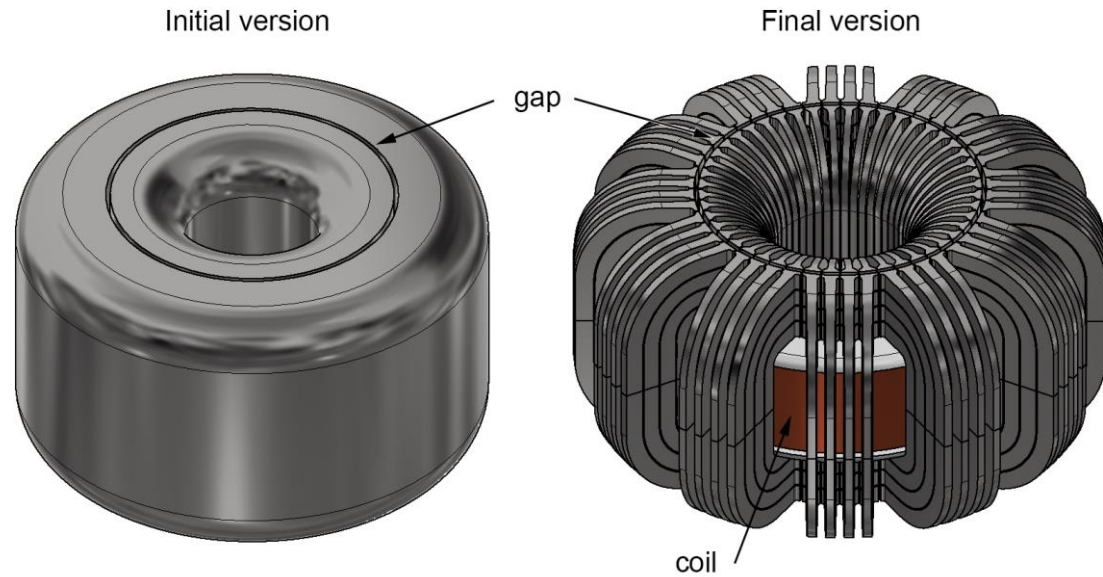
MR valve design

The magnetic circuit evolution

- Number of grooves
- Shape of grooves

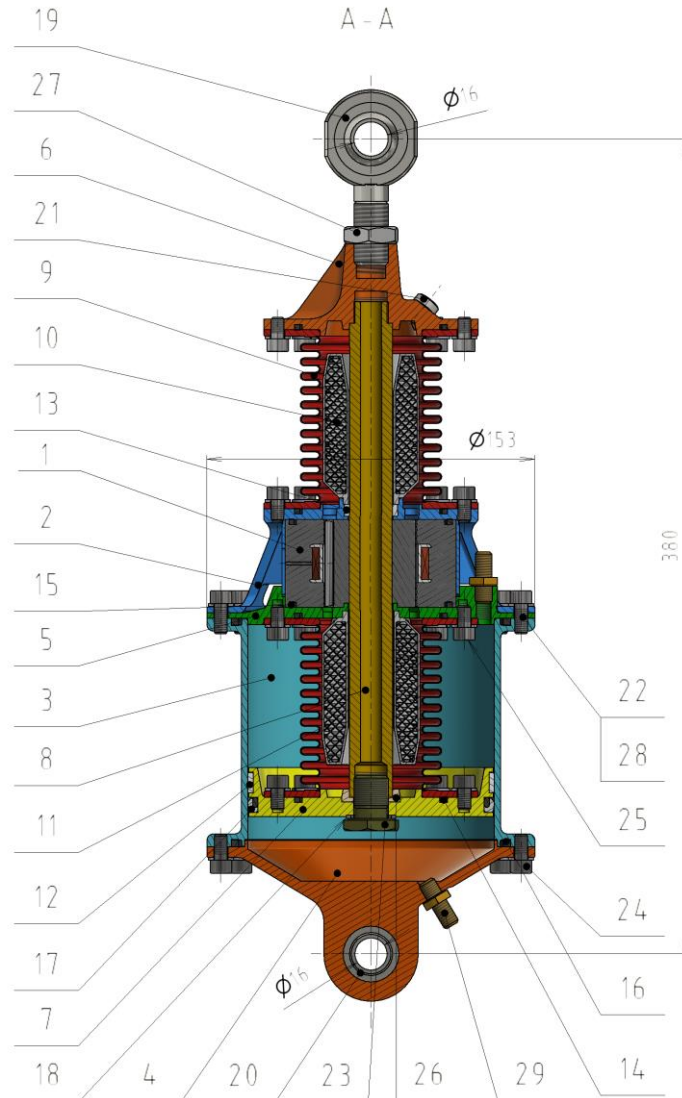


MR valve design



Version	Weight [kg]	Outer diameter [mm]	Primary time response [ms]	Secondary time response [ms]	Intensity of mag. field in the gap [kA/m]
Initial	1.184	69	3.84	15 (approx.)	264
Final	0.632	80	0.38	0.65	251
Difference	-46.6%	+15.9%	-94.3%		-4.6%

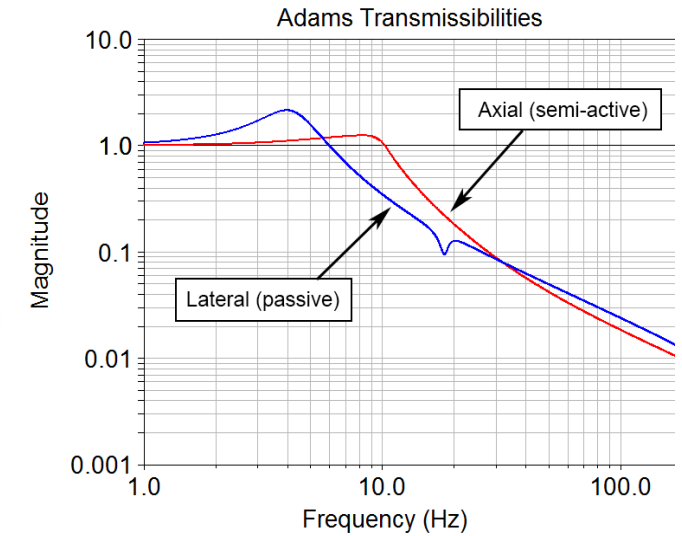
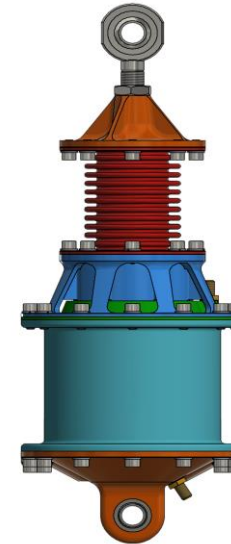
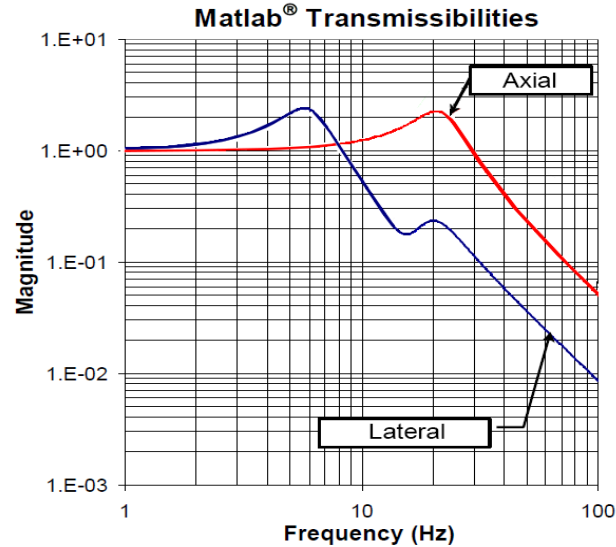
MR strut design



Pos.	Name of part	Material	Weight [g]	Quantity
1	MR valve	Vacoflux / Lukopren / cooper	693	1
2	MR valve body	AZ80A-T5 (magnesium alloy)	169	1
3	Cylinder	AZ80A-T5	337	1
4	Lid	AZ80A-T5	385	1
5	Flange	AZ80A-T5	159	1
6	Adapter	Ti6Al4V (titanium alloy)	279	1
7	Piston	AZ80A-T5	176	1
8	Piston rod	Ti6Al4V	230	1
9	Bellows	1.4571 (stainless steel)	447	2
10	Upper stopper	AZ80A-T5	49	1
11	Lower stopper	AZ80A-T5	48	1
12	Piston guideline	PTFE	2	1
13	Piston rod guideline	PTFE	11	1
14	Seal 66x2.5	NBR	1	4
15	Seal 71x2.5	NBR	2	2
16	Seal 123x3.4	NBR	4	2
17	Piston seal	NBR / PTFE	9	1
18	Bonded seal	NBR / Steel	2	1
19	Rod end M81935/1	Ti6Al4V	127	1
20	Lower mount	Ti6Al4V	16	1
21	Plug	AZ80A-T5 / NBR	2	1
38	Screw M6x16	Ti6Al4V	4	12
23	Piston rod screw	Ti6Al4V	23	1
24	Screw M6x12	Ti6Al4V	3	12
25	Screw M6x10	Ti6Al4V	3	32
26	Washer	Ti6Al4V	8	1
27	Nut	Ti6Al4V	12	1
28	Split washer 6.4	Ti6Al4V	0.4	56
29	Taxer valve	C-360 (brass alloy)	9	2
	MR Fluid	MR 122 EG	443	186 ml

Total strut mass **4.145 kg**

MR sturt vs ELVIS strut

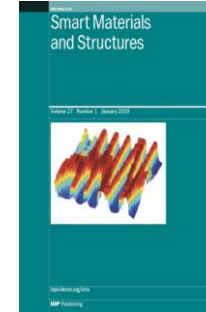


Strut	Payload mass [kg]	Weight of strut [kg]	Tramissibility at natural frequency (axial) [-]	Tramissibility at 5x natural frequency (axial) [-]
ELVIS	1135	7.71	2.2 (20 Hz)	0.05 (100 Hz)
MR	1500	4.15	1.2 (8 Hz)	0.05 (40 Hz)
Difference	+32.1%	-53.8%	-45%	0%

Conclusion

Two versions of MR strut were designed

- Experimental – tests were published



3rd review

- For the launch vehicle – better then ELVIS strut:

load capacity

+ 32 %

weight

- 46 %

transmissibility

- 45 %

Method of the pressure thrust stiffness determination was created



3D print -> magnetic circuit with time response much faster than the MR fluid



Thank you for your attention

Ondřej Macháček

ondrej.machacek@vutbr.cz



INSTITUTE OF MACHINE
AND INDUSTRIAL DESIGN

www.ustavkonstruovani.cz